

**A COMPUTATIONAL CHEMISTRY STUDY ON  
THE INTERACTIONS BETWEEN  
HYDROGENATED BOROPHENE AND AMINO  
ACIDS**

**A Thesis Submitted to  
the Graduate School of Engineering and Sciences of  
İzmir Institute of Technology  
in Partial Fulfillment of the Requirements for the Degree of**

**MASTER OF SCIENCE**

**in Chemistry**

**by  
Yağmur BOZKURT**

**July 2022  
İZMİR**

## ACKNOWLEDGEMENT

I can not be the only lead of this thesis. I took precious help from important people in my life. I need to show my biggest gratitude to my supervisor Prof. Dr. Nuran Elmacı Irmak, without her sincere patience, support, and essential guidance, completing this thesis wouldn't be possible.

I also want to remark that to be a part of IZTECH and Elmacı Research Group was an excellent pleasure and my biggest pride.

I'd like to thank my research group members, especially Fethi Can Demirci and Mustafa Coşkun Özdemir who were always there for my questions.

I would like to extend my deepest gratitude to Prof.Dr. Elif Işgın and Dr. Onur Büyükçakır for their valuable advices and reviews.

My family is the foundation of my personality and morality. I want to thank my Peker Family, my best friends, and Mon Trésor for supporting my academic career and for making me shielded to protect from depression.

I owe great gratitude to the ones I sent to heaven; my grandparents Kemal and Ayşen Peker and my angel best friend Cennet Kınacı. I can feel your prayers from heaven for my success.

This Thesis is dedicated to my mother, Saniye Peker, who endured my heavy rains and rainbows.

## ABSTRACT

### A COMPUTATIONAL CHEMISTRY STUDY ON THE INTERACTIONS BETWEEN HYDROGENATED BOROPHENE AND AMINO ACIDS

In this work, the adsorption behavior of hydrogenated borophene to amino acids was examined to provide its geometric and electronic structures information and to check whether hydrogenated borophenes' potential can be used in new biosensor devices for amino acids or not. In the aspect of this thesis adsorption of 4 amino acids from different types of amino acid classes (acidic, basic, nonpolar, and polar) on hydrogenated borophene surfaces has been studied by computational chemistry methods.

Electronic and geometric structures of  $B_{36}H_6$  and its complexes with glycine, tyrosine, aspartic acid, and histidine were obtained by DFT calculations at B3LYP-D2 / 6-311G\*\* level of theory. In the energetically most favorable configurations of complexes, amino acids approaching from the bottom of the  $B_{36}H_6$  surface with a horizontal orientation (exception for histidine complexes) of amino acid was observed. The most reactive parts of the  $B_{36}$  structure (edges) have been stabilized with hydrogenation, the whole boron cluster became more stable and adsorption ability has fallen.

It was found that hydrogenated borophene has indistinguishable electronic responses for each the amino acids studied in this thesis since the complexes exhibited nearly the same band gap. Thus, hydrogenated borophene shows no sensor ability to GLY, TYR, ASP, and HIS.

## ÖZET

### HİDROJENLENMİŞ BOROFEN VE AMİNO ASİTLER ARASINDAKİ ETKİLEŞİM ÜZERİNE HESAPLAMALI KİMYA ÇALIŞMASI

Bu tez çalışmasında, hidrojenlenmiş borofenin amino asitlere karşı adsorpsiyon davranışı, geometrik ve elektronik yapı bilgilerini sağlamak ve hidrojenlenmiş borofenlerin amino asitler için yeni biyo-sensör cihazlarında kullanılma potansiyeli incelenmiştir. Bu tez kapsamında, farklı amino asit sınıflarından (asidik, bazik, polar olmayan ve polar) 4 amino asidin hidrojenlenmiş borofen yüzeylerine adsorpsiyon davranışları hesaplamalı kimya yöntemleri ile çalışılmıştır.

$B_{36}H_6$  ve glisin, tirozin, aspartik asit ve histidin ile komplekslerinin elektronik ve geometrik yapıları, B3LYP-D2 / 6-311G\*\* teorisi seviyesinde DFT hesaplamaları ile elde edilmiştir. Enerjisel olarak en uygun kompleks konfigürasyonlarında,  $B_{36}H_6$  yüzeyinin alt konumunda amino asitlerin yatay bir yönelim (histidin kompleksleri hariç) ile yaklaştığı gözlemlenmiştir.  $B_{36}$  yapısının en reaktif kısımları (kenarlar) hidrojen eklenmesi ile daha stabilize olarak tüm bor kümesi daha kararlı hale gelmiştir ve adsorpsiyon kabiliyeti düşmüştür.

Hidrojenlenmiş borofenin, bu tezde çalışılmış amino asitler üzerinde ayırt edilemez elektronik tepki gösterdiği gözlemlenmiştir. Her bir amino asit –  $B_{36}H_6$  kompleksi için neredeyse aynı HOMO-LUMO enerji farkı elde edilmiştir.

Bu nedenle hidrojenlenmiş borofenin, GLY, TYR, ASP ve HIS amino asitleri için sensör yeteneği olduğu söylenemez.

# TABLE OF CONTENTS

LIST OF FIGURES .....	vi
LIST OF TABLES.....	vii
LIST OF ABBREVIATIONS .....	viii
CHAPTER 1. INTRODUCTION .....	1
1.1. Definition, History and Properties of Borophene and Hydrogenated Borophene .....	1
1.2. Amino Acid definition and importance .....	5
1.3. Literature Work .....	6
1.3.1. Theoretical Studies .....	6
1.3.2. Synthesis Studies .....	10
1.4. Aim of the study .....	11
CHAPTER 2. METHODS & MATERIALS.....	13
2.1. Conformational Analysis .....	13
2.2. Frequency Calculations .....	13
2.3. DFT Calculations .....	14
2.4. Computational aspects of the study .....	16
CHAPTER 3. RESULTS & DISCUSSION.....	17
3.1. Method Validation .....	18
3.2. Conformational Analysis .....	18
3.3. DFT Results .....	19
3.4. Global indices .....	25
CHAPTER 4. CONCLUSION .....	28
REFERENCES .....	29
APPENDICES	
APPENDIX A .....	33
APPENDIX B .....	45

# LIST OF FIGURES

<b><u>Figure</u></b>	<b><u>Page</u></b>
Figure 1.1 Structures of monoelemental 2D nanomaterials .....	2
Figure 1.2 Historical survey of Borophene structures .....	3
Figure 1.3 The synthesis methods to grow 2D nanomaterials .....	4
Figure 1.4 Amino Acid Classification .....	5
Figure 1.5 a) Glycine's structure and labelled orientation points, b) Tyrosine's structure and labelled orientation points, c) Aspartic Acid's structure and labelled orientation points, d) Histidine's structure and labelled orientation points .....	6
Figure 1.6 Structure of B <sub>36</sub> H <sub>6</sub> .....	6
Figure 1.7 a) possible position points on $\chi^3$ borophene b) DNA nucleobases structures .....	9
Figure 1.8 Different Adenin / B <sub>36</sub> complexes .....	9
Figure 1.9 Positioning of DNA sequences through graphene and Borophene nanopores .....	9
Figure 1.10 The configuration the system .....	10
Figure 2.1 Jacob's Ladder approach .....	16
Figure 2.2 a) possible location points of attachment to the surface of Borophene structure b) orientation points of Amino acids to the Borophene surfaces .....	17
Figure 3.1 Structures of B <sub>36</sub> and B <sub>36</sub> H <sub>6</sub> .....	19
Figure 3.2 NBO charges of a) B <sub>36</sub> H <sub>6</sub> and b) B <sub>36</sub> . .....	20
Figure 3.3 Band Gap energy differences between complex and B <sub>36</sub> H <sub>6</sub> . .....	23
Figure 3.4 NBO charges of B <sub>36</sub> H <sub>6</sub> - Amino acid complexes a)Glycine b)Tyrosine c)Aspartic Acid .....	25
Figure 3.5 NBO charges of B <sub>36</sub> H <sub>6</sub> - Amino acid complexes a)Histidine (CO orientation) b)Histidine (NH <sub>2</sub> orientation) .....	25

## LIST OF TABLES

<b><u>Table</u></b>	<b><u>Page</u></b>
Table 3. 1 Energy values and CPU time values of performed calculations. ....	18
Table 3. 2 Bond distances between the atoms of B <sub>36</sub> and B <sub>36</sub> H <sub>6</sub> .....	20
Table 3. 3 HOMO, LUMO energies and Band Gap (BG) of B <sub>36</sub> and B <sub>36</sub> H <sub>6</sub> in eV .....	20
Table 3. 4 Structures, HOMO and LUMO energies and shapes, Band gap (BG), Band gap differences between complex and B <sub>36</sub> H <sub>6</sub> ( $\Delta$ BG), and Fermi level energy (Ef). .....	24
Table 3. 5 Global indices values for complexes of Glycine. ....	26
Table 3. 6 Global indices values for complexes of Tyrosine. ....	27
Table 3. 7 Global indices values for complexes of Aspartic Acid. ....	27
Table 3. 8 Global indices values for complexes of Histidine. ....	27

## LIST OF ABBREVIATIONS

2D	Two Dimensional
DFT	Density Functional Theory
NEGF	The Non-Equilibrium Green Function (NEGF) method
B3LYP	Becke-3-parameter-Lee–Yang–Parr Functional
PBE	Perdew-Burke-Ernzerhof Functional
DNA	Deoxyribonucleic Acid
GGA	Generalized Gradient approximation
LDA	The Local Density Approximation
AA	Amino Acid
BG	Band Gap
$\Delta$ BG	Band Gap Difference
% $\Delta$ BG	Percentage of Band Gap Difference
NBO	Natural Bond Orbitals
HOMO	Highest Occupied Molecular Orbital
LUMO	Lowest Unoccupied Molecular Orbital
ESP	Electrostatic Potential



# CHAPTER 1

## INTRODUCTION

### 1.1. Definition, History and Properties of Borophene and Hydrogenated Borophene

Borophene is a two-dimensional (2D) nanomaterial formed by boron atoms that belong to the 3A element group in the periodic table. Boron is known as the only nonmetal and semiconductor element in its group. Boron has an electron configuration of  $1s^1 2s^2 2p^1$  and holds an  $sp^2$  hybridized orbital. By means of orbital features, boron atoms act much like carbon atoms.

Generating new 2D materials from 3A, 4A, and 5A elements from the periodic table of elements drew huge attention after graphene's discovery. Its properties are worth superlative adjectives. Construction by one element favors easy and rapid metabolization in biological systems. Simple synthesis could be provided since they are produced in a mono-elemental way. These 2D nanomaterials can be used in conductor applications because their main elements are semiconductors. Thanks to the characteristics listed previously, 2D mono-elemental nanomaterials may be outstanding. The newly proposed 2D nanomaterials have properties like large surface areas and physiochemical activities which ensured them materials to be applied in supercapacitors, hydrogen storage, bioimaging, drug carries, bio-like materials, biosensors, and other electronic devices. The discovered nanomaterials were named after the atoms they are made up of, such as; Silicene, Germanene, Stanene, Phosphorene, Arsenene, Antimonene, Bismuthene, and Borophene (Figure 1.1).

There are numerous different Borophene structures. These structures are named based on their unique patterns. The nomenclature of boron cluster structures can be categorized under three classes; i) Distorted hexagonal (DH) plane, ii) buckled triangular (BT) plane, and iii) mixed triangular-hexagonal (MTH) plane. Distorted hexagonal planes (Figure 1.2 Hexagonal structure) are constituted as quasi-planar structures by hexagon units just like graphene. Buckled triangular planes (Figure 1.2 buckled structure (namely 2-Pmmn)) are constructed by repeating  $B_7$  pyramidal structures while MTH planes are created by hollow hexagon structures and triangular

patterns. In another naming principle for mono-elemental 2D materials, they can be classified according to their specific coordination numbers; (when CN is 5 or 6)  $\alpha$ -type, (when CN is 4, 5, or 6)  $\beta$ -type, (when CN is 4 or 5)  $\chi$ -type, (when CN is a single number)  $\delta$ -type and (when CN is 3, 4 or 5)  $\psi$ type. DH and BT planes can be categorized under  $\delta$ -type planes; conversely, MTH planes can be sorted by any planes with the exclusion of  $\delta$ -type planes (Ou, et al. 2021).

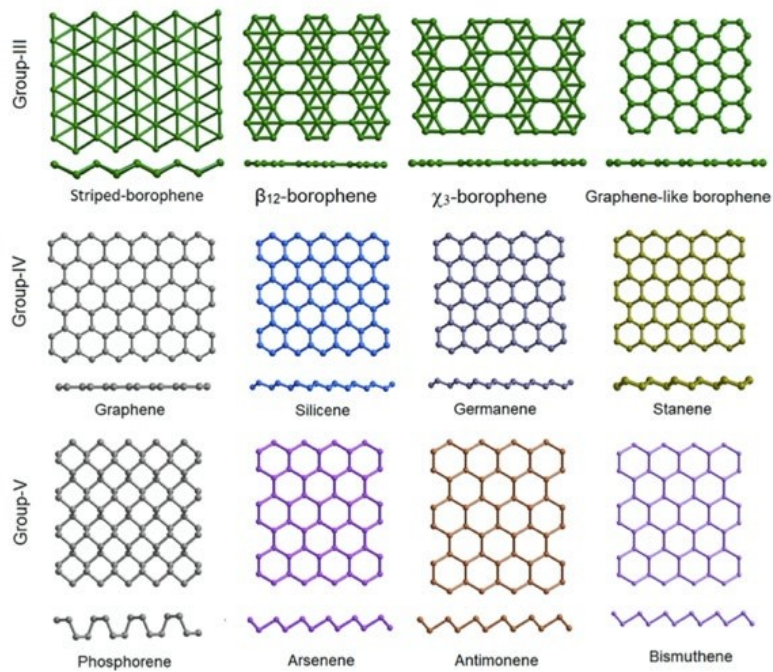


Figure 1. 1 Structures of mono-elemental 2D nanomaterials  
(Source: Vishnoi, 2019)

Differences in composition and pattern lead to distinct properties. For example;  $\beta_{12}$ -type Borophene exhibits anisotropic features (Zhou, et al. 2017) when  $\alpha$ -type shows isotropic features (Xiao, et al. 2017) . 2-Pmmn phase has boron atoms in a zig-zag direction. However, it does have a negative Poisson's ratio. High anisotropy and larger

The Young's modulus than graphene can be observed (Wang, et al. 2019)

The existence of Borophene nanosheets started with a theoretical study (Boustani 1995) which has succeeded to predict quasi-planar-shaped boron clusters. This article has been followed by future studies. Kuntsmann and Ouandt (Kuntsmann and Quandt 2006) explained the basic buckled structures of 2D boron nanosheets by Aufbau Principle. In the period that buckled structure is known as the most stable

boron cluster, another study (Tang and Beigi 2007) predicted  $\alpha$ -sheet structure would be a more favorable type of boron sheet with lower energy. The next inspiring study (Wang, Zhang and Lin 2014) described the concept of Borophene and proved that Borophene structures with hexagonal holes like  $B_{36}$  were exceptionally stable among others.

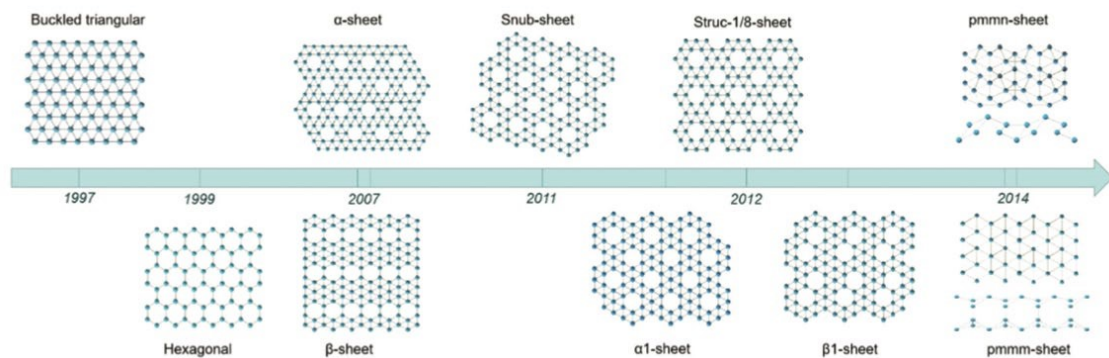


Figure 1.2 Historical survey of Borophene structures  
(Source: Ou et al., 2021)

Even though the theoretical studies on Borophene have developed, the synthesis of Borophene sheet has not been accomplished until 2015 (Mannix, et al. 2015) (Feng, et al. 2016). Borophene synthesis has been performed in two main principles; Bottom-up and Top-down (Figure 1.3) (Ou, et al. 2021). For the bottom-up synthesis approach, Borophene sheets have been developed on different surfaces such as Ag(111), Cu(111), Au(111), and Cu foils when the top-down methods have been done by using Boron powders.

Boron cluster's light masses are caused by strong bonding between atoms. Strong anisotropy of the structure and extraordinary phonon transmission result in possessing superior thermal conductance even higher than graphene.

Borophene's low mass density favors both superconductivity and fast phonon transport at extremely high temperatures (by the good electron-phonon coupling). Borophene can be used as an adoption in composite designs due to its great strength and in-plane hardness. It also could be utilized in flexible nanodevices thanks to its high elasticity against off-plane deformation.

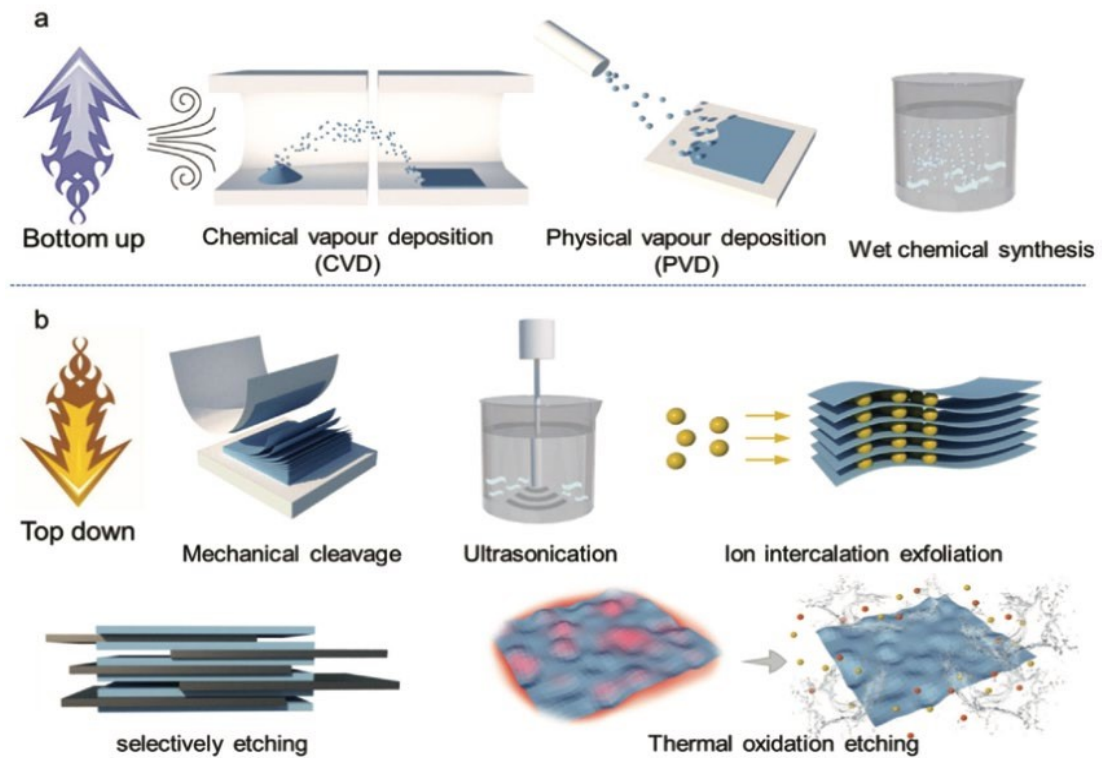


Figure 1.3 The synthesis methods to grow 2D nanomaterials  
(Source: Ou, 2021)

Two-dimensional boron sheets have delocalized bonds by multiple hexagonal holes. The atoms of these parts behave like electron donors which leave the edges of borophene poor of electrons causing inertness to oxidation (Tang and Beigi, Self-doping in boron sheets from first principles: A route to structural design of metal boride nanostructures 2009). It is known that borophene is a promising supreme nanomaterial, but it is unlikely to implement due to its obvious predisposition for oxidation in an inert environment. Since the edges are active points that are open to oxidation, the scientists proposed adding hydrogen atoms to each edge. This hypothesis has been proved by studies made in Chen's team (Chen, et al. 2014). Thus, hydrogen bonds worked as electron acceptors. Hydrogenation made the nanosheet more stable and demonstrated superlative electronic and mechanical properties (Hou, et al. 2020). These additives also could turn superconductor material into semiconductor materials. High conductance is not a desired feature for sensor applications. Hence, in this thesis, we aimed to observe hydrogen addition's effect on the conductance.

To summarize, an increase in hydrogen bonds causes; expanding surface area which would result in decreasing the tension, and a decrease in hardness. It is observed that bending stiffness and Poisson's ratio are directly connected to the density of hydrogen bonds. After these critical studies, we have seen that we could attune 2D nanomaterials' properties by rearranging the concentration of hydrogen bonds.

## 1.2 Amino Acid definition and importance

Amino acids are organic compounds that can be identified as monomer units of protein chains. Each amino acids have an amino ( $-\text{NH}_3^+$ ) and a carboxylate ( $-\text{CO}_2^-$ ) group besides each other's unique side chains (R group) attached to their central carbon atom. They do not contain other elements except Carbon (C), Hydrogen (H), Oxygen (O), Nitrogen (N), and Sulphur (S). Amino acids can be categorized into classes according to their properties such as; charge, hydrophilicity, hydrophobicity, size, or functions. The most common classification is based on polarity and charge (Figure 1.4).

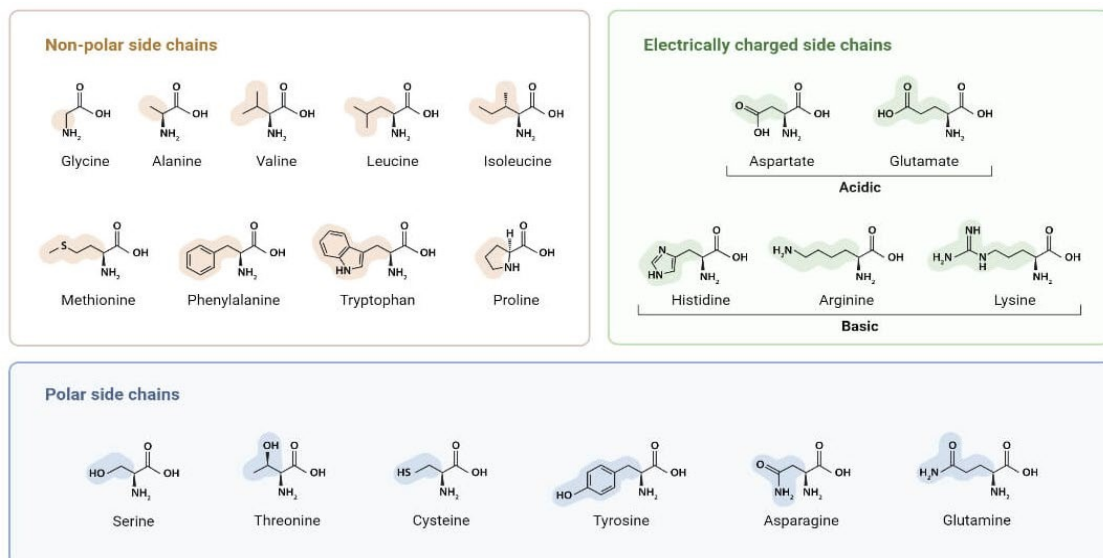


Figure 1.4 Amino Acid Classification Reprinted from "Amino Acid Chart  
(Source: URL1.)

Proteins' functions originated from the sequencing of amino acids. Amino acids essentially build up; muscle structure, nervous system functions, Important organs' health and attributing to the cellular formation in human body.

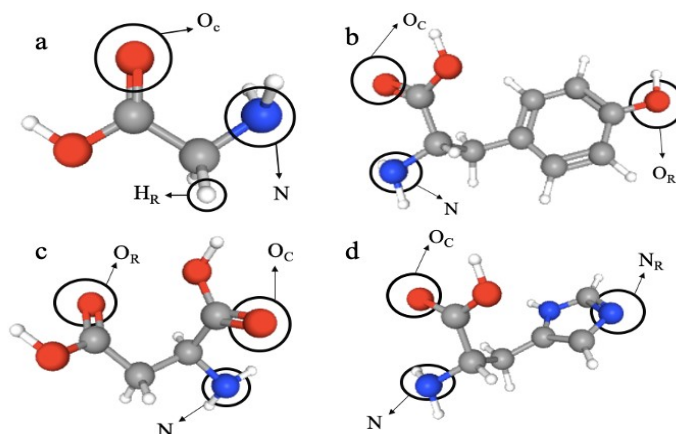


Figure 1.5 a) Glycine’s structure and labelled orientation points, b) Tyrosine’s structure and labelled orientation points, c) Aspartic Acid’s structure and labelled orientation points, d) Histidine’s structure and labelled orientation points

## 1.3 Literature Work

### 1.3.1 Theoretical Studies

In the study conducted by Chen et al. in 2014 the stability of different structures of Borophene and hydrogen-doped isomers was compared with energy calculations using the PBE0 functional and the 6-311+G\* base set, and it was observed that the honeycomb  $B_{36}$  borophene structure had the lowest energy. Based on this, the effect of hydrogen addition to  $B_{36}$  on the molecular structure was also investigated and it was found that both structures had concentric triple aromatic properties. In addition, borophene in the hydrogenated  $B_{36}H_6$  form, which was first proposed in that work (Figure 1.6) (Chen, et al. 2014) is the subject of this thesis.

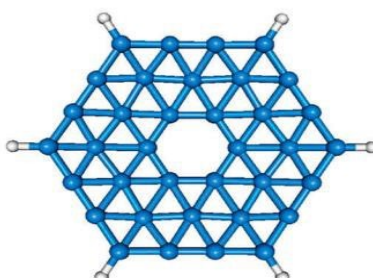


Figure 1.6 Structure of  $B_{36}H_6$   
(Source: Chen, 2014)

According to the phonon distribution calculations carried by Xu et al., while Borophene gives virtual frequencies, hydrogenated virtual frequencies do not. In this

way, hydrogenated Borophene has been shown to be dynamically more stable (Xu, Du and Kou 2016).

Calculations regarding the density of partial states have shown that there is a strong orbital hybridization between the s orbital of hydrogen atoms and the  $p_z$  orbital of boron atoms (Wang, Lü, et al., New crystal structure prediction of fully hydrogenated borophene by first principles calculations 2017).

Shao et al. were stated that hexagon-shaped hydrogenated Borophenes, called  $\delta_3$  and  $\delta_5$ , have an ideal use in nanostructures by performing calculations at the DFT level of theory (Shao, et al. 2019).

In the experimental and computational study of Sang et al., it has been suggested that semiconductor hydrogenated Borophene can be used in field effect transistors at nanoscale (Sang, et al. 2021).

In the current literature, the adsorption ability of Borophene against gas molecules has been studied with DFT calculations such that; atmospheric gas (Hossain et al., 2020), toxic cyanogen gas (Rahimi and Solimannejad 2018), ammonia (Rostami and Soleymanabadi 2016), cyanogen halide (Tayebi and Shojaie 2021), Ozone (Tahmasebi, Biglari and Shakerzadeh 2017), formaldehyde and many molecules such as acetaldehyde-propanal (Mohsenpour, Shakerzadeh and Zare 2017), Acrolein (Allal, et al. 2020), and CO/CO<sub>2</sub> (Arefi, Horri and Tavakoli 2021).

In the study conducted by Shukla et al., it was shown that the adsorption of CO, NO, NO<sub>2</sub> or NH<sub>3</sub> gases on the Borophene surface is much stronger than graphene, MoS<sub>2</sub> and phosphorene. The large change in the transmission functions of Borophene after adsorption and ON and OFF states in the sensor mechanism reveal the sensor potential (Shukla, et al. 2017). An electronic sensor capability of Borophene for formaldehyde was investigated, it was found that the homo-lumo difference of B<sub>36</sub> molecule decreased by 69% with the effect of formaldehyde, and as a result of DFT calculations (Shahbazi Kootenaei and Ansari 2016).

The adhesion of the anti-cancer drug fluorouracil (FU) on Borophene with DFT methods was studied, the oxygen of the FU molecule tends to attach to the edge of B<sub>36</sub> with a noticeable adsorption energy. They showed that the edges of the Borophene molecule are more reactive towards the FU molecule. At the same time, B<sub>36</sub>-FU complexes were investigated in aqueous solutions and suggested that these complexes with high polarity would be good candidates for drug delivery

(Shakerzadeh 2017). In another drug sensor study, Vessally and colleagues examined the adsorption behavior of B<sub>36</sub> Borophene for the drug cisplatin. Their calculations have shown that; the molecule is captured from the corner position of Borophene by the Cl and H atoms in its structure (Vessally, et al. 2020). Borophene adsorbing efficiency on metronidazole was observed with DFT calculations. It was revealed that the corner part of Borophene adsorbed the NO<sub>2</sub> group of the drug. Borophene may be said to be promising as a drug sensor (Xiao, et al. 2020).

Amino acids play a vital role in biological systems, as they are the building blocks of proteins. For this reason, having an inside look at the amino acid sequence of a protein is very important in order to understand the biological function of that protein and even to find solutions to some diseases. In the literature below, some studies on Borophene structures' adsorbing ability with biological structures will be given.

In 2020, a study that involve Adenine nucleobase's adsorption behavior on  $\chi_3$  Borophene 2D nanosheet has been published (Sabokdast, et al. 2020). Three types of the orientation of nucleobases structure on different positions of Borophene surface were examined. Outcomes demonstrated high adsorption energy and charge transfer which strengthen the probability of Borophene's usage in DNA sequence detecting devices.

By taking action from the previous study, the same team has extended their research focus to cover all of the DNA nucleobases (Adenine, Cytosine, Guanine, and Thymine). This time, density functional theory (DFT) and non-equilibrium Green's function (NEGF) have been performed together to have a closer look at the electronic properties of nucleobases and  $\chi_3$  Borophene complexes with parallel and perpendicular orientation (Figure 1.7) (Sabokdast, Horri, et al., Detection of nucleobases on Borophene Nanosheet: A DFT investigation 2021). The results showed that the ( $E_{lumo}-E_{homo}$ ) band gap decreased by proof of an increase in electrical conductivity. It is possible to identify each DNA nucleobase by a device that has Borophene as sensing material.

In a study by Rastgou and his team, the interactions of the nucleobases that make up the DNA chain with Borophene were investigated by DFT calculations (Figure 1.8). The conductivity sensitivity of Borophene to cytosine, guanine, adenine, and thymine is  $C > T > A \sim G$ , while the order of the effect of nucleobases on reactivity



is shown as  $A > G > C > T$ . In accordance with the results, it was revealed that cytosine has the strongest signal and each nucleobase can be distinguished (Rastgou, Soleymanabadi and Bodaghi 2017).

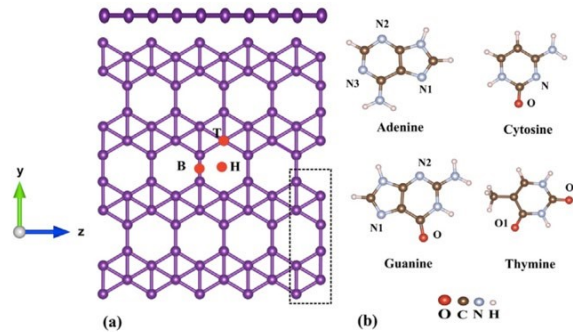


Figure 1. 7 a) possible position points on  $\chi_3$  borophene b) DNA nucleobases structures  
(Source: Sabokdast, 2020)

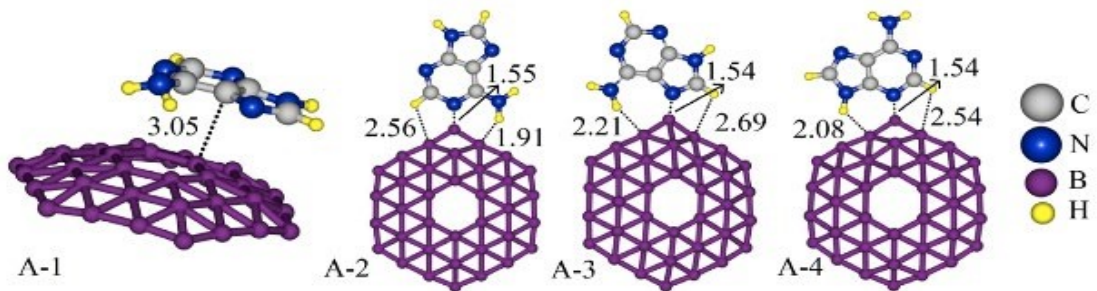


Figure 1.8 Different Adenine /  $B_{36}$  complexes  
(Source: Rastgou, 2017)

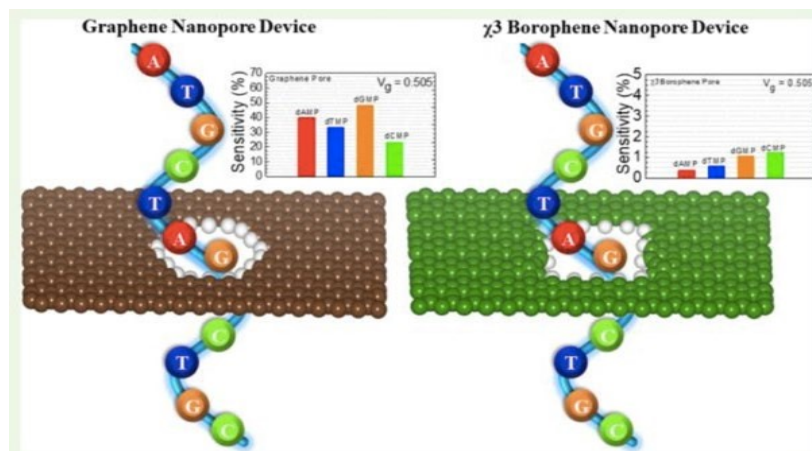


Figure 1. 9 Positioning of DNA sequences through graphene and Borophene nanopores  
(Source: Jena, 2021)

In another study, DFT studies were carried out to examine the potential applications of both the graphene thin layer and the DNA sequence of X3 Borophene. Molecules are brought close to the sheet, as the DNA sequence is passed through a pore in the sheet. (Figure 1.9). DFT and NEGF were used for transverse conductivity studies. The results showed that; While both nanomaterials give good results, graphene has more potential than Borophene (Jena, Kumawat and Pathak 2021).

In the study by Rodríguez and his team, a device consisting of graphene that can act as an amino acid sensor was modeled (Figure 1.10). When a potential between 1V and 2V is applied, it was observed that the modeled device showed a high degree of selectivity and sensitivity for the amino acids Histidine, Alanine, Aspartic acid and Tyrosine (Rodríguez, Makinistian and Albanesi 2017).

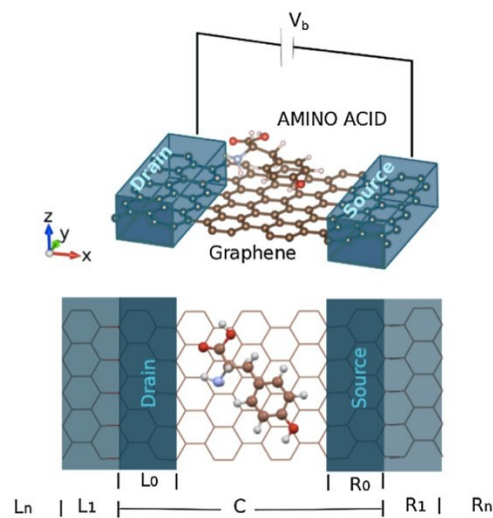


Figure 1. 10 The configuration the system

(Source: Rodríguez, 2017)

### 1.3.2 Synthesis Studies

Synthesis of Borophene can be accomplished by Bottom-up and Top-down methods as shown in Figure 1.3. There are many studies based on the bottom-up technique.

The most common Borophene growing strategy is based on using silver plates. Guisinger et al. have succeeded in the synthesis of thin 2D Borophene on a clean silver

surface which contributed to a good inert environment for boron monolayer growth (Mannix, et al. 2015). This study resulted in two different phases of Borophene nanosheets; the homogenous phase (higher deposition rate) and the striped phase (low deposition rate).

Wu et al. used a synthetic pathway to grow  $\beta_{12}$  (570-650 K) and  $\chi_3$  (650-800K) phase Borophene structures on Ag(111) substrate with high vacuum (Feng, et al. 2016).

Another research team of Zhong used Ag(110) to synthesize Borophene nanoribbons (BNR). Four phases were observed; labeled as P1, P2, P3, and P4 with different lattice constants (Zhong, et al. 2017).

The Usage of copper is another option for the synthesis. According to a study in 2015, Borophene (pnm characteristics) was produced on the copper foil (Tai, et al. 2015). Gozar's research team made a study to compare Ag(111) and Cu(111) surfaces' characteristics in the means of Borophene synthesis. Outcomes have stated that Cu(111) was better than Ag(111) due to its less inertness, higher conductivity, and ability to result in larger single Borophene crystals (Wu, et al. 2019).

Al(111) was also been used for Borophene growth. The study obtained a linear hexagonal honeycomb Borophene structure which have Dirac characteristics just like graphene (Li, et al. 2018).

Guisinger's team has also used Au(111) to grow Borophene by thermal deposition. To separate Borophene from the surface was easy due to the weak bonding between Au(111) and boron atoms (Kiraly, et al. 2019).

## **1.4 Aim of the study**

In this project, the interaction of amino acids with hydrogenated Borophene which is one of the graphene-like materials will be investigated to provide preliminary information and to design new biosensor materials using computational chemistry methods. Although there are a few similar studies focused on the adsorption of amino acids on graphene, silicene, and phosphorene surfaces in the current literature, there is no such study with Borophene to our knowledge.

In the scope of this project physical/chemical adsorption of 4 amino acids from different types of amino acid classes on hydrogenated Borophene, surfaces will be studied. Electronic and most favored geometric structures will be revealed with calculations at the DFT level of theory. Along with the in-depth analysis of the calculations to be made, it will be determined whether Borophene has a special response behavior to a specific amino acid functional group or aromaticity, polarity, etc. Also, hydrogenated Borophene's sensitivity order for amino acids will be revealed. The results of the project will support, inspire and guide experimental studies for applications such as drug delivery, electronics, and biosensors of Borophene-like materials, as well as in the synthesis of Borophene.

## CHAPTER 2

### METHODS & MATERIALS

#### 2.1 Conformational Analysis

The conformational study is an essential part of molecular studies to get information about stability, Physico-chemical features, and activities. Most molecules might have multi-low energy conformations. Conformational analysis is done to study unique conformations of a molecule or cluster in means of three-dimensional changes caused by rotation through  $\sigma$  bonds. We need to know all variants and the lowest energy conformations to commend the structure and reactivity. We expect the conformations to be distributed according to Boltzmann distribution. Molecular mechanics calculation methods enable us to see all/most possible conformers with their relative energy values. This method works by rotating molecules through rotation centers by taking steric interactions, torsional and angle strains into account. The algorithm rotates the molecule by the chosen number of step sizes to get new conformers to minimize the energy repeatedly until finding the lowest energetic molecule.

#### 2.2 Frequency Calculations

Performing frequency calculations is critical in computational chemistry to characterize the stationary structures by finding vibrational and harmonic frequency values. It is also used to get vibrational zero point corrected energies and thermodynamics information of the system of interest. Zero point corrected energies are obtained by adding zero point energies to the electronic energies. Frequencies might provide insights for IR spectroscopic measurements and pre-information about transition state, saddle points, and global – local minimum points of the conformations.

The harmonic vibrational frequency calculation can be used to provide thermochemical properties. Frequency calculations are rational only when they are performed on the already optimized structure. Default conditions are accepted as 298.15K for temperature, 1 atm for pressure, and principle isotope for each element type; unless the desired conditions were specified on the input file.

$$\text{Sum of electronic \& zero point energy } E_0 = E_{\text{elec}} + \text{ZPE} \quad (1)$$

$$\text{Sum of electronic \& thermal energy } E = E_0 + E_{\text{vib}} + E_{\text{rot}} + E_{\text{trans}} \quad (2)$$

Frequency calculation also contributes to the understanding of stationary states. Essentially, optimization provides convergence of structure on PES when intermolecular and extra molecular forces are zero (mutual-stabilized). Outcomes enlighten scientists on whether the optimized structure is a stationary state, saddle point, local or global minimum point. Also, the direction of the minimum point can be designated.

## 2.3 DFT Calculations

Density Functional Theory is a type of quantum mechanics calculation method that can be used on a comprehensive list of systems from molecules to crystals. DFT might be performed with Non-Equilibrium Green's Function (NEGF) to investigate electronic instrument systems. It can compute properties without empirical values. Low computational cost and relatively high accuracy provided the DFT method a reputation. DFT is most used in research areas, such as; organic chemistry, inorganic chemistry, metallurgy, material engineering, ceramics science, etc. DFT made a tremendous impact in computational physics and chemistry its establishment.

Schrödinger's equation in the N-body system is still a problematic phenomenon that is impossible to solve for systems with more than one electron. Employ different approximations is the only way to get closer to the solution.

Since it is not easy to use wavefunction ( $\Psi$ ) to get to the solution\*, the DFT approximation takes advantage of electron probability ( $\rho$ ) as a function with respect to space and time. This feature accelerates the computation (Because  $\Psi$  has 3N variables for the N atom system when  $\rho$  has only x,y, and z coordinates). Hohenburg

and Kohn also contributed to the popularity of DFT methods by their statement that computing via electron density supplies all information about the ground state that is needed.

Density Functional Theory has become the most extensively used technique for quantum chemical calculations thanks to its benefits such as; low computation cost, shorter computing time and even better matching with empirical values. The distinctive feature of this method is the utilization of electron density instead of the wavefunction.

The essential information that a scientist needs to know is electron distribution (density) and electronic energy. Electron density can give details about dipole moment (polarity) and charge distribution. By Born - Oppenheimer approximation applied, potential energy surface can be obtained, revealing energies of different molecular geometries and bond energy barriers.

In 1925, Erwin Schrödinger presented his worldly-known equation (named after him, the Schrödinger equation) to explain wave function theory. This theory focuses on the wave function. The solution to the wave function requires more equations that are too complicated to solve.

$$H\Psi = E\Psi \quad (3)$$

$$E = \min_{\Psi} \langle \Psi | H | \Psi \rangle \quad (4)$$

The energy (E) of the system is estimated by minimization of the expectation value of the Hamiltonian (H) as given in equation (4), it is explained the minimizing method to approach electronic energy according to Wave Function Theory.

After this dilemma, in 1965 Hohenberg and Kohn proposed a two-part theorem that build The Density Functional Theory as an accurate computation technique. These theorems employ the ground-state density and the density of the system itself with Molecular Orbital Theory.

$$E = \min_n \{ \int V_{\text{nuclei}}(r\vec{r})n(r\vec{r})d^3r\vec{r} + F[n(r\vec{r})] \} \quad (5)$$

In equation (5), according to DFT, n stands for density and F stands for universal functional.

Later on that year, Kohn continued his work with Sham and created the Kohn-

Sham system which accepts ground state density as the same density as the real system.

$$E = T + V_{ne} + V_{ee} + V_{xc} \quad (6)$$

In equation (6), T stands for non-interacting kinetic energy,  $V_{ne}$  for Coulomb interaction with nuclei, and  $V_{ee}$  for Coulomb interaction of electron density  $\rho$  with itself.

Different functionals are grouped in accordance with the approximations they obey. The Local Density Approximation (LDA) accepts that the whole system has one density. Although LDA functionals could provide good geometries, the obtained energy values aren't very accurate compared to other functionals. To correct this inaccuracy, Generalized Gradient approximations (GGA) were created. This corrects the connection between density changes through different coordinates. Jacob's Ladder helps us to understand the improvement of functional groups and to decide which functional would fit our calculation (Figure 2.1).

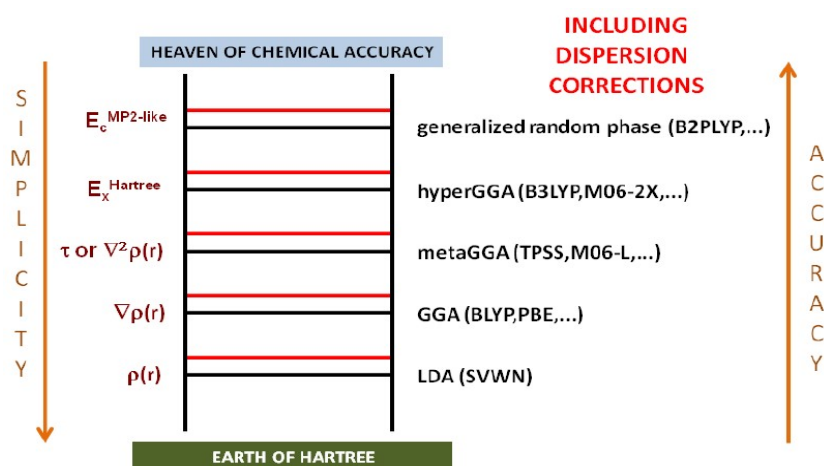


Figure 2. 1 Jacob's Ladder approach (Source:Gomes, 2013)

Band gaps values are used to investigate interaction between structures of the complexes. Band gap energy can be calculated by the following equation (7).

$$BG = E_{LUMO} - E_{HOMO} \quad (7)$$

$$\Delta BG = BG_{complex} - BG_{B36H6} \quad (8)$$

$$\% \Delta BG = ( \Delta BG / BG_{B36H6} ) \times 100 \quad (9)$$



## 2.4 Computational aspects of the study

In this study, hydrogenated Borophene's electronic structure, equilibrium geometry, and structural stability have been computed by using DFT methods. All calculations have been carried out at B3LYP-D2 / 6-311G\*\* level of theory. Several software has been used for different calculation types, including; Spartan10 for conformational study, PSI4 v1.5.0 for optimization, Gaussian09 for frequency calculations, and Avogadro for visualization.

One amino acid has been chosen from each amino acid group; glycine as an apolar AA, Tyrosine as a polar AA, Aspartic acid as an acidic AA, and Histidine as a basic AA. By this means, a total of 4 amino acid-Hydrogenated Borophene complexes have been formed. Placing amino acids on the Borophene surface from different places (in Figure 2.2.a, indicated by the red arrow); different configurations of the complexes were designed and studied with approximations from 3 different groups of amino acids (by amino group, carboxyl group, and functional group; as shown in Figure 2.2.b).

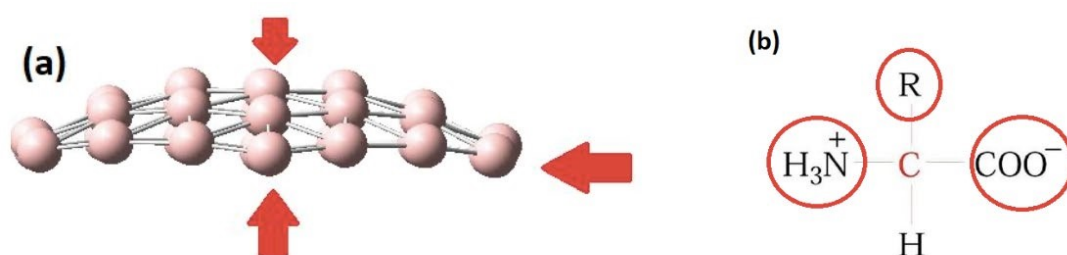


Figure 2.2 a) possible location points of attachment to the surface of Borophene structure. b) orientation points of Amino acids to the Borophene surfaces

## CHAPTER 3

### RESULTS & DISCUSSION

#### 3.1 Method Validation

A methodology for DFT calculations on hydrogenated Borophene has been designed according to the trial calculations' results. Recent literature has demonstrated that functionals like 'Becke-3-parameter-Lee-Yang-Parr' (B3LYP), 'Perdew-BurkeErnzerhof' (PBE), and WB97X-D and basis sets like 6-31G, 6-311G and 6-31G\* were the most common and suitable functional/basis sets for Borophene optimization. Based on this information, numerous calculations with different combinations of basis sets have been performed.

Functionals	Basis sets	Energy values (kJ/mol)	CPU time (with 20 cores) Day-Minute:Second
B3LYP-D2	6-31G**	-2357742,58	00-29:22
	6-311G**	-2358101,874	01-20:46
	6-31+G**	-2357801,388	01-22:28
B3LYP-D3	6-31G**	-2357469,335	00-23:11
	6-311G**	-2357828,202	01-16:29
	6-31+G**	-2357526,793	01-46:49
PBE MBJ	6-31G**	-2354794,231	00-30:32
	6-311G**	-2355111,137	02-35:03
	6-31+G**	-2354833,653	00-46:04
WB97X-D	6-31G**	-2356484,967	02-40:24
	6-311G**	-2356825,216	01-24:10
	6-31+G**	-2356607,42	03-35:20

Table 3. 1 Energy values and CPU time values of performed calculations.

As seen in Table 3.1; by putting the lowest energy and affordable time, we have decided to continue further calculations with B3LYP-D2 \ 6-311G\*\* basis set.

## 3.2 Conformational Analysis

We did a conformational analysis for each amino acid to be examined. For this purpose, Spartan10 software was used to perform a conformation search. Each amino acid gave us a different number of conformers based on the number of their torsional centers; 11 conformers for Glycine, 431 conformers for Tyrosine, 431 conformers for Aspartic acid, and 35 conformers for Cysteine. For equilibrium energy calculations, the level of theory has increased (from Semi-empirical (AM1 to PM6) to Hartree Fock (631G)) as we decreased the number of conformers (from maximum number to 10). After taking the conformers and energy values from this study, We applied principal component analysis to obtain a diverse and small sized conformations sample, to be input of the energy optimization at DFT B3LYP-D2 / 6-311G\*\* level of theory. The final conformers have been tested by the frequency calculations to ensure that they are true minima (if they have zero imaginary frequency). Complex studies have been designed after this part.

## 3.3 DFT Results

Before complex studies, examinations on  $B_{36}$  and  $B_{36}H_6$  structures have been done to accomplish a good comparison between the electronic properties of these two clusters. The favorable structures of both Borophenes obtained at B3LYP-D2/6-311G\*\* level of theory are displayed in Figure 3.1.

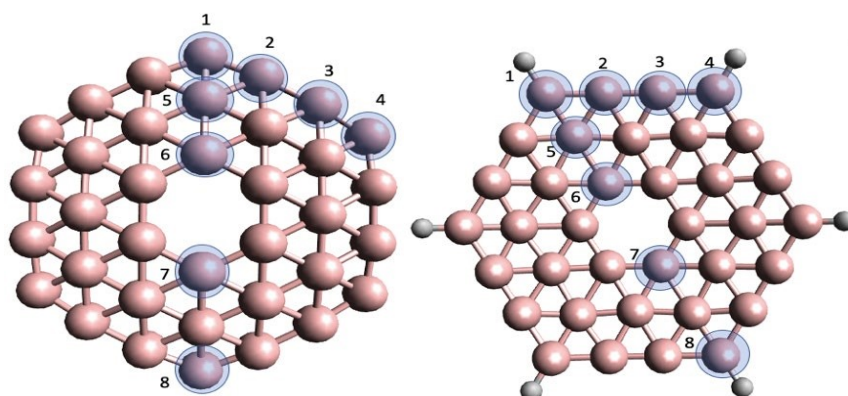


Figure 3.1 Structures of  $B_{36}$  and  $B_{36}H_6$

Structures	Distances (Å)						
	1 – 2	2 – 3	1 – 4	1 – 5	5 – 6	6 – 7	1 – 8
B <sub>36</sub>	1,575	1,67	4,779	1,638	1,725	3,309	9,557
B <sub>36</sub> H <sub>6</sub>	1,693	1,593	4,968	1,615	1,822	3,232	9,935

Table 3.2 Bond distances between the atoms of B<sub>36</sub> and B<sub>36</sub>H<sub>6</sub>

	B <sub>36</sub> H <sub>6</sub>	B <sub>36</sub>
HOMO	-5,92229	-5,8997
LUMO	-3,60388	-3,95708
BG	2,318411	1,942622

Table 3.3 HOMO, LUMO energies and Band Gap (BG) of B<sub>36</sub> and B<sub>36</sub>H<sub>6</sub> in eV

Bond lengths of B<sub>36</sub> and B<sub>36</sub>H<sub>6</sub> have been given in Table 3.2 according to the atoms chosen and shown in Figure 3.1. Hydrogen addition enlarged the Borophene surface by about 0.4 Å since an increase in edges ( $\sim 0.5$  Å), and an increase in diameter of honeycomb structure measured through the distance between B1 and B8 atom ( $\sim 0.4$  Å).

The curvature of the Borophene surface decreased by hydrogenation according to the examination dihedral angle labeled as 8–D–4–1 (D is a dummy atom at the center of the surface). This dihedral angle changed from 148.9° to 160.9° upon the addition of hydrogens to B<sub>36</sub>, the surface became flatter.

Adding H-atoms to Borophene destabilized the LUMO energy while HOMO energy left almost the same. Eventually, this caused an increase in the HOMO LUMO difference (BG), which makes the cluster less conductive.

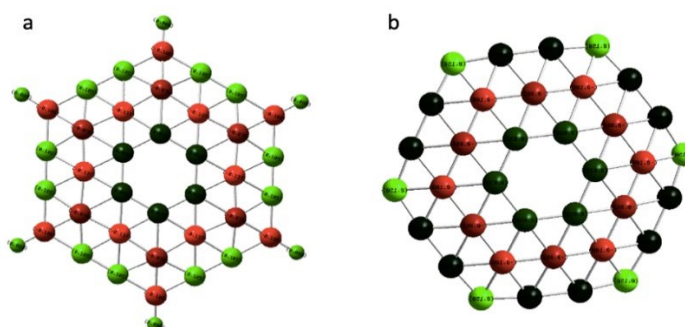


Figure 3.2 NBO charges of a) B<sub>36</sub>H<sub>6</sub> and b) B<sub>36</sub>.

NBO analyses have been performed to obtain the charges of atoms in B<sub>36</sub> and B<sub>36</sub>H<sub>6</sub>. It was observed that positive charges are located on the boron atoms between edges and on the hydrogen atoms in the B<sub>36</sub>H<sub>6</sub> cluster. Negative charges are seen on boron atoms in middle hexagon and boron atoms at the corners of outer hexagon. The central hexagon has been observed totally neutral. By the comparison between NBO charges of B<sub>36</sub>H<sub>6</sub> and B<sub>36</sub>, it is seen that hydrogen addition affected mostly the outer hexagon's charge distributions. The atom charges at the corners of the edges on the surface where H-atoms are bonded turned from most positive to most negative value while two Boron atoms located in the middle of each edge became much positive via Hydrogen addition.

Hydrogenated Borophene's adsorption ability for amino acids (Glycine, Tyrosine, Aspartic Acid, and Histidine) have been investigated by using Density Functional Density Theory calculations. DFT optimization calculations were performed with the B3LYPD2/6-311G\*\* basis set which is implemented via PSI4 1.5 software.

To understand the features of hydrogenated Borophene as an adsorbent, it is recommended to focus on adsorption energy (Complexation energy).

$$E_{\text{ads}} = E_{\text{complex}} - (E_{\text{B}_{36}\text{H}_6} + E_{\text{aa}}) + \text{BSSE} \quad (10)$$

$E_{\text{ads}}$  stands for adsorption energy which can be calculated by the equation (10). The sum of zero point corrected energies of B<sub>36</sub>H<sub>6</sub> and amino acid is subtracted from the complex's zero point corrected energy. Adding The Basis Set Superposition Error (BSSE) value up to the total calculation prevents this error.

Frequency calculations have been carried out to investigate the local and global minima points. A few imaginary frequencies have been obtained from calculations. To prevent imaginary frequencies and getting closer to a minimum point, the 'manual displacement' option has been used that is implemented in Gaussian09 software. Outputs proved that minimum point complex structures were in a good match with our chosen energetically favorable complexes.

We are going to do a comparison in two parts; an orientation comparison for each amino acid & comparison among those four amino acids for the most likely complex conformation.

The results in Table B.1, Table B.3, Table B.5, and Table B.7, demonstrated that energetically the most favorable complexes for each amino acid group have been

found as; Gly-Bottom-CO for Glycine AA, Tyr-Bottom-NH<sub>2</sub> for Tyrosine, Asp-Bottom-NH<sub>2</sub>, and His-Bottom-CO.

The followings were observed for the geometric features of the most favorable complexes. Glycine is located in a horizontal position on the B<sub>36</sub>H<sub>6</sub> surface with 2.9 Å and 3.2 Å distances from CO and NH<sub>2</sub> groups respectively.

Tyrosine is the other amino acid that is placed parallel to the surface of B<sub>36</sub>H<sub>6</sub>. The closest group of amino acids is the amino moiety with distances of 1.7 Å and 2.5 Å from hydrogen and nitrogen atoms. The carboxylate and functional groups are near the surface of hydrogenated Borophene by 3.1 Å and 2.6 Å, respectively.

Aspartic Acid structure is approached to the Borophene surface in a horizontal manner. The amino group's hydrogen and nitrogen atoms are 1.5 Å and 2.5 Å away from the surface. The other parts of the amino acid have been docked to the surface about 3.5 Å.

The only vertical orientation of amino acid to the surface was detected in the Histidine complex. The amino acid was placed facing carboxylate (C=O), hydroxyl (OH attached to carboxylate), and the amino group (-NH<sub>2</sub>) to the adsorbent. While the smallest distance was 2.4 Å between carboxylate oxygen and Borophene, the distances of 2.7 Å and 3.3 Å have been obtained by hydroxyl and amino groups, respectively.

Another conformer of histidine complex which has very close energy (energy difference is 0,00262 kJ/mol) to the most likely one (Bottom-CO) was determined in which Histidine's amino group was orientated from the bottom location. For that configuration, the amino acid structure has approached horizontally with distances of 1,538 Å from the hydrogen atom and 2,424 Å from the nitrogen atom of the amino group to the surface. As a natural consequence of horizontal docking, carboxylate (3,44 Å) and the functional groups (2,89 Å) are the other close parts of amino acid to the surface.

The second most stable conformer for glycine complexes has 1,60 kJ/mol relative energy. In this structure, the carboxylate group approach from the top part and optimization resulted in reversed curvature (convex to concave) of the honeycomb structure which looked similar to the bottom configuration. The next ranked favorable structure is oriented from the functional group to the top location with relative energy of 21.45 kJ/mol.

For tyrosine, the second and the third most likely structures are both on top location with -NH<sub>2</sub> (16,24 kJ/mol) and -CO (23,60 kJ/mol) groups respectively.

Aspartic acid complexes have two configurations that are close energetically to each other and have higher energy than the most favorable configuration by 17,35 kJ/mol (Top-NH<sub>2</sub>) and 17,69 kJ/mol (Bottom-CO).

The three most stable configurations of histidine complexes are located on the bottom position of hydrogenated Borophene. The energies of Bottom-NH<sub>2</sub> and BottomCO complexes are almost the same.

The structures, frontier orbitals and their energies for the most stable configurations are given in Table 3.4. In each complex, both HOMO and LUMO orbitals have no electron density on amino acid structures (Figure 3.4 and exclusively in Figure A.1 to Figure A.36). All complex systems have nearly the same HOMO and LUMO orbital shapes. In HOMO, the electron density is evenly distributed on outer hexagons; while in LUMO we observed an electron migration from outer hexagons towards the inner hexagon. Electrons are delocalized generally. Nodes are present in HOMO and LUMO.

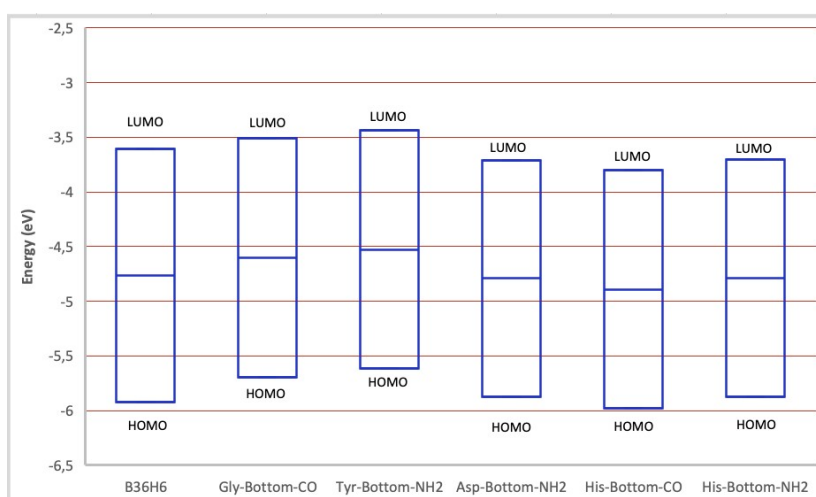


Figure 3.3 Band Gap energy differences between complex and B<sub>36</sub>H<sub>6</sub>.

The most likely structures of complexes of each amino acid have been compared in Table 3.4, Figure 3.2 and exclusively in Table B.2, Table B.4, Table B.6, and Table B.8; The HOMO LUMO differences for all aa-complexes are similar so do percentages of BG differences which measures the sensitivity (see Table 3.4). It seems that hydrogenated Borophene has almost the same electronic response to these amino acids. Hydrogenated Borophene does not have sensor potential towards these amino acids according to these results.

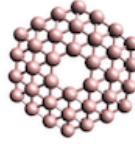
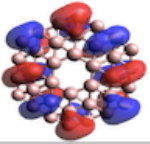
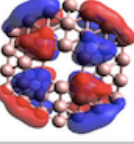
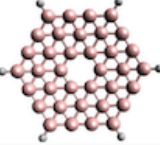
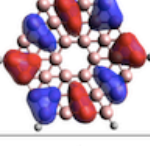
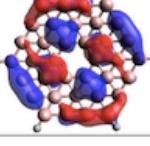
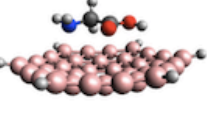

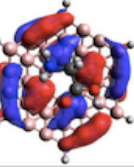
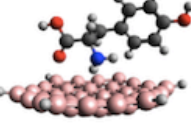
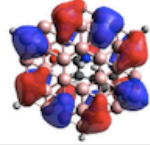
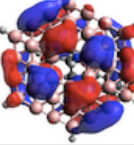
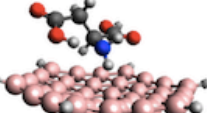
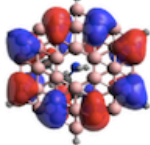
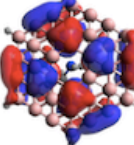
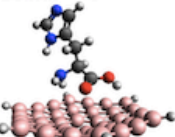
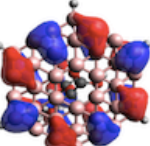
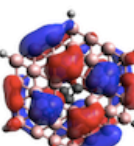
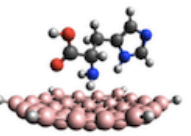
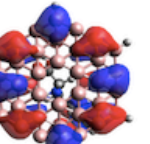
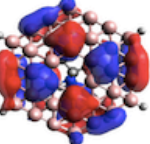
Structure	HOMO	LUMO	BG (eV)	$\Delta$ BG (eV)	Eads (kJ/mol)	Ef (eV)
B36 	-5,900 	-3,957 	-1,943	-	-	-6,907
B36H6 	-5,922 	-3,604 	2,318	-	-	-4,763
Gly - Bottom - CO 	-5,698 	-3,511 	2,187	-0,131	-75,020	-4,604
Tyr - Bottom - NH2 	-5,617 	-3,436 	2,182	-0,137	-81,144	-4,526
Asp - Bottom - NH2 	-5,872 	-3,710 	2,162	-0,157	-79,207	-4,791
His - Bottom - CO 	-5,980 	-3,805 	2,175	-0,143	-64,649	-4,892
His - Bottom - NH2 	-5,871 	-3,707 	2,164	-0,155	-64,646	-6,952

Table 3.4 Structures, HOMO and LUMO energies and shapes, Band gap (BG), Band gap differences between complex and B<sub>36</sub>H<sub>6</sub> ( $\Delta$ BG), and Fermi level energy (Ef).



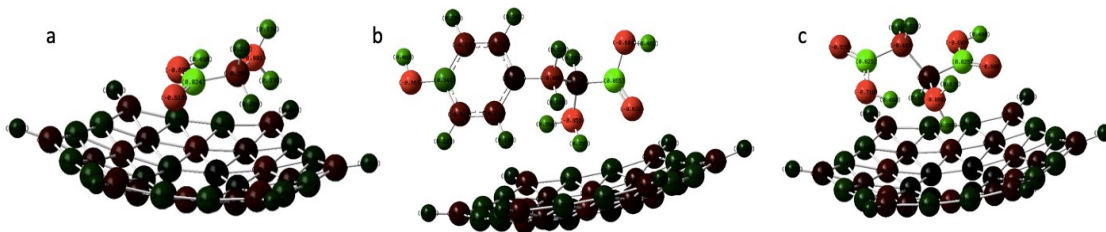


Figure 3. 2 NBO charges of B<sub>36</sub>H<sub>6</sub> - Amino acid complexes a)Glycine b)Tyrosine c)Aspartic Acid

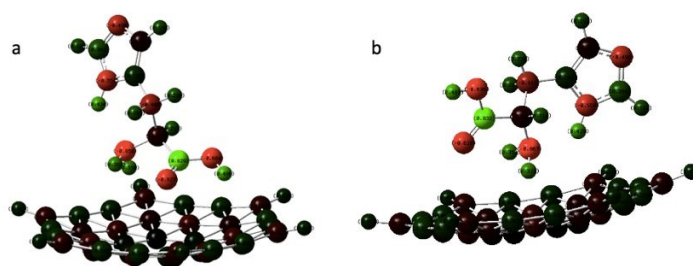


Figure 3. 3 NBO charges of B<sub>36</sub>H<sub>6</sub> - Amino acid complexes Histidine a) CO orientation b) NH<sub>2</sub> orientation

The common fact that was derived from complexes' NBO charge is shown in Figure 3.4 and Figure 3.5 with colors (light green to light red scales most positive to most negative charge ranges) and ESP (electrostatic potential) (see Figure A.1 to Figure A.36) visualization is that the whole B<sub>36</sub>H<sub>6</sub> structure is neutral. The central carbon atoms of amino acids have been observed as nearly neutral.

Among all those calculations, the most favorable location of hydrogenated Borophene for amino acid adsorption has been determined as the bottom (concave) position.

### 3.4 Global indices

Global indices such as; chemical Potential ( $\mu$ ), Hardness ( $\eta$ ), Softness ( $S$ ), and electrophilicity ( $\omega$ ) have been calculated to enlighten the important features of 2D nanomaterials. All the equations below have been used to calculate these parameters. All we need is the energy values of the highest occupied molecular orbital (HOMO) and lowest unoccupied molecular orbital.

Chemical Potential

$$\mu = \frac{E_{HOMO} + E_{LUMO}}{2} \quad (11)$$

Hardness  $\eta = \frac{E_{LUMO} - E_{HOMO}}{2}$  (12)

Softness  $S = \frac{1}{2\eta}$  (13)

Electrophilicity  $\omega = \frac{\mu^2}{2\eta}$  (14)

Fermi Level Energy  $E_f = E_{HOMO} - [(E_{LUMO} - E_{HOMO}) / 2]$  (15)

When we consider Table 3.5, Table 3.6, Table 3.7, and Table 3.8; there is not a respectable difference between complexes. Even though hydrogenated Borophene exhibits a good amount of hardness and electrophilicity for many applications, comparing this parameter among the complexes is not very conceivable due to the incomparable outcomes.

It is known that higher chemical potential means higher reactivity (Vessally, et al. 2020). By leading on this information; we can say the Tyrosine-Bottom-NH2 complex has the highest chemical potential -4,526 eV and the highest reactivity among others.

	Position	Orientation	The Chemical Potential (eV)	Hardness (eV)	Softness (1/eV)	The Electrophilicity (eV)	Ef (eV)
<b>G l y c i n e</b>	<b>Edge</b>	-Co	-4,479	1,106	0,452	9,068	-6,691
		-NH2	-4,648	1,107	0,452	9,757	-6,863
		-R	-4,701	1,113	0,449	9,931	-6,927
	<b>Top</b>	-Co	-4,626	1,085	0,461	9,858	-6,797
		-NH2	-4,732	1,116	0,448	10,036	-6,963
		-R	-4,685	1,118	0,447	9,817	-6,920
	<b>Bottom</b>	-Co	-4,604	1,094	0,457	9,693	-6,792
		-NH2	-4,667	1,090	0,459	9,994	-6,847
		-R	-4,845	1,070	0,467	10,968	-6,984

Table 3. 5 Global indices values for complexes of Glycine.

	Position	Orientation	The Chemical Potential (eV)	Hardness (eV)	Softness (1/eV)	The Electrophilicity (eV)	Ef(eV)
T y r o s i n e	Edge	-Co	-4,590	1,111	0,450	9,481	-6,812
		-NH2	-4,547	1,105	0,452	9,355	-6,758
		-R	-4,776	1,113	0,449	10,244	-7,002
	Top	-Co	-4,532	1,119	0,447	9,182	-6,769
		-NH2	-4,549	1,122	0,445	9,220	-6,794
		-R	-4,789	1,108	0,451	10,347	-7,005
	Bottom	-Co	-4,633	1,078	0,464	9,958	-6,788
		-NH2	-4,526	1,091	0,458	9,391	-6,708
		-R	-4,759	1,096	0,456	10,334	-6,950

Table 3. 6 Global indices values for complexes of Tyrosine.

	Position	Orientation	The Chemical Potential (eV)	Hardness (eV)	Softness (1/eV)	The Electrophilicity (eV)	Ef(eV)
A s p a r t i c  A c i d	Edge	-Co	-4,488	1,107	0,452	9,097	-6,702
		-NH2	-4,789	1,113	0,449	10,307	-7,014
		-R	-4,741	1,111	0,450	10,118	-6,963
	Top	-Co	-4,383	1,132	0,442	8,489	-6,647
		-NH2	-4,726	1,094	0,457	10,210	-6,913
		-R	-4,787	1,120	0,447	10,234	-7,026
	Bottom	-Co	-4,972	1,092	0,458	11,318	-7,156
		-NH2	-4,791	1,081	0,463	10,618	-6,952
		-R	-4,432	1,097	0,456	8,951	-6,626

Table 3. 7 Global indices values for complexes of Aspartic Acid.

	Position	Orientation	The Chemical Potential (eV)	Hardness (eV)	Softness (1/eV)	The Electrophilicity (eV)	Ef(eV)
H i s t i d i n e	Edge	-Co	-4,708	1,110	0,450	9,981	-6,928
		-NH2	-4,777	1,111	0,450	10,273	-6,999
		-R	-4,514	1,107	0,452	9,205	-6,727
	Top	-Co	-4,752	1,120	0,446	10,081	-6,992
		-NH2	-4,769	1,107	0,452	10,276	-6,983
		-R	-4,455	1,113	0,449	8,919	-6,681
	Bottom	-Co	-4,892	1,087	0,460	11,005	-7,067
		-NH2	-4,789	1,082	0,462	10,598	-6,952
		-R	-4,493	1,090	0,459	9,264	-6,672

Table 3. 8 Global indices values for complexes of Histidine.

## CHAPTER 4

### CONCLUSION

In this thesis, the adsorption of amino acids with hydrogenated Borophene was examined to provide primary outcomes and to check hydrogenated Borophenes' ability to be used in new biosensor devices for amino acids using computational chemistry methods. In the content of this study physical/chemical adsorption of 4 amino acids from different types of amino acid classes (acidic, basic, nonpolar, and polar) on hydrogenated Borophene surfaces was investigated.

Electronic and geometric structures of  $B_{36}H_6$  and its complexes with glycine, tyrosine, aspartic acid, and histidine were obtained by DFT calculations at the B3LYPD2 / 6-311G\*\* level of theory. In the most favored configurations of complexes, docking from the bottom of the  $B_{36}H_6$  surface with a parallel orientation (except histidine complexes) of amino acid was observed. The most electron acceptor parts of the  $B_{36}$  structure (edges) have been inhibited with hydrogen addition, the boron cluster became less reactive and adsorption ability decreased as expected.

It was observed that hydrogenated Borophene has almost the same electronic response to the amino acids studied in this work since the complexes possessed nearly the same band gap. Thus hydrogenated Borophene has no sensor ability towards GLY, TYR, ASP, and HIS.

For future studies, this project will continue with expanding amino acid lists to a total of 12 amino acids to examine the adsorption behavior.

## REFERENCES

- Allal, H., Y. Belhocine, S. Rahali, M. Damous, and N. Ammouchi. 2020. "Structural, electronic, and energetic investigations of acrolein adsorption on B36 borophene nanosheet: A dispersion-corrected DFT Insight." *Journal of Molecular Modeling* 26 (6).
- Arefi, V., A. Horri, and M. B. Tavakoli. 2021. "Transport properties of na-decorated borophene under CO/CO<sub>2</sub> adsorption." *Computational and Theoretical Chemistry*.
- Boustani, I. 1995. "Structure and stability of small boron clusters. A density functional theoretical study." *Chemical Physics Letters* 240 (1-3): 135-140.
- Chen, Q., G. Wei, W. Tian, H. Bai, Z. Liu, H. Zhai, and S. Li. 2014. *Quasi-planar aromatic b36 and b36-clusters: All-boron analogues of coronene*. Vol. 16. 34 vols. Physical Chemistry Chemical Physics.
- Feng, B., J. Zhang, Q. Zhong, W. Li, S. Li, H. Li, P. Cheng, S. Meng, L. Chen, and K. Wu. 2016. *Experimental realization of two-dimensional boron sheets*. Vol. 8. 6 vols. Nature Chemistry.
- Hou, C., G. Tai, J. Hao, L. Sheng, B. Liu, and Z. Wu. 2020. *Ultrastable crystalline semiconducting hydrogenated borophene*. Vol. 59. 27 vols. Angewandte Chemie International Edition.
- Jena, M. K., R. L. Kumawat, and B. Pathak. 2021. "First-principles density functional theory study on graphene and borophene nanopores for individual identification of DNA nucleotides ." *ACS Applied Nano Materials* 4 (12).
- Kiraly, B., X. Liu, L. Wang, Z. Zhang, A.J. Mannix, B. L. Fisher, B. I. Yakobson, M. C. Hersam, and N. P. Guisinger. 2019. "Borophene Synthesis on Au(111)." *ACS Nano* 13 (4).
- Kunstmann, J., and A. Quandt. 2006. "Broad boron sheets and boron nanotubes: An ab initio study of structural, electronic, and mechanical properties." *PHYSICAL REVIEW B* 74 (2).
- Li, W., L. Kong, C. Chen, J. Gou, S. Sheng, W. Zhang, H. Li, L. Chen, P. Cheng, and K. Wu. 2018. "Experimental realization of honeycomb borophene." *Science Bulletin* 63 (5).

- Mannix, A. J., X. F. Zhou, B. Kiraly, J.D. Wood, D. Alducin, B. D. Myers, X. Liu, et al. 2015. *Synthesis of borophenes: Anisotropic, two-dimensional boron polymorphs*. Vol. 350(6267). 1513-6 vols. *Science*.
- Mohsenpour, Z., E. Shakerzadeh, and M. Zare. 2017. "Quantum Chemical Description of formaldehyde (HCHO), acetaldehyde (CH<sub>3</sub>CHO) and Propanal (CH<sub>3</sub>CH<sub>2</sub>CHO) pollutants adsorption behaviors onto the bowl-shaped B36 nanosheet." *Adsorption* 23 (7-8).
- Ou, M., X. Wang, L. Yu, C. Liu, W. Tao, and X. Ji. 2021. "The emergence and evolution of borophene." *Advanced Science* 8 (12).
- Rahimi, R., and M. Solimannejad. 2018. "Can bowl-like B30 nanostructure sense toxic cyanogen gas in air?: A theoretical study." *Molecular Physics* 116 (17).
- Rastgou, A., H. Soleymanabadi, and A. Bodaghi. 2017. "DNA sequencing by Borophene nanosheet via an electronic response: A theoretical study." *Microelectronic Engineering* 169 (15-16).
- Rodríguez, S., L. Makinistian, and E. Albanesi. 2017. "Graphene for amino acid biosensing: Theoretical study of the electronic transport." *Applied Surface Science* 419.
- Rostami, Z., and H. Soleymanabadi. 2016. "N–H bond cleavage of ammonia on graphene-like B36 borophene: DFT Studies." *Journal of Molecular Modeling* 22 (4).
- Sabokdast, S., A. Horri, Y. T. Azar, M. Momeni, and M. B. Tavakoli. 2021. "Detection of nucleobases on Borophene Nanosheet: A DFT investigation." *Bioelectrochemistry* 138.
- Sabokdast, S., A. Horri, Y. T. Azar, M. Momeni, and M.B. Tavakolia. 2020. "Adsorption of adenine molecule on borophene nanosheets: A density functional theory study." *Physica E: Low-dimensional Systems and Nanostructures* 119.
- Sang, P., Q. Wang, W. Wei, Y. Li, and J. Chen. 2021. "Hydrogenated borophene as a promising two-dimensional semiconductor for nanoscale field-effect transistors: A computational study." *ACS Applied Nano Materials* 4 (11).
- Shahbazi Kootenaei, A., and G. Ansari. 2016. "B36 borophene as an electronic sensor for formaldehyde: Quantum Chemical Analysis." *Physics Letters A* 380 (34).

- Shakerzadeh, E. 2017. "Quantum Chemical Assessment of the adsorption behavior of Fluorouracil as an anticancer drug on the B 36 nanosheet." *Journal of Molecular Liquids* 240.
- Shao, L., X. Duan, Y. Li, Q. Yuan, B. Gao, H. Ye, and P. Ding. 2019. "A theoretical study of several fully hydrogenated borophenes." *Physical Chemistry Chemical Physics* 21 (14).
- Shukla, V., J. Wörnå, N. K. Jena, A. Grigoriev, and R. Ahuja. 2017. "Toward the realization of 2D borophene based gas sensor." *The Journal of Physical Chemistry C* 121 (48).
- Tahmasebi, E., Z., Biglari, and E. Shakerzadeh. 2017. "In silico investigation of the ozone (O<sub>3</sub>) binding behavior to the B36 bowl-shaped structure." *Adsorption* 23 (6).
- Tai, G., T. Hu, Y. Zhou, X. Wang, J. Kong, T. Zeng, Y. You, and Q. Wang. 2015. "Synthesis of Atomically Thin Boron Films on Copper Foils." *Angew Chem Int Ed Engl* 54 (51).
- Tang, H., and S.I. Beigi. 2007. "Novel Precursors for Boron Nanotubes: The Competition of Two-Center and Three-Center Bonding in Boron Sheets." *PHYSICAL REVIEW LETTERS* 99 (11).
- . 2009. *Self-doping in boron sheets from first principles: A route to structural design of metal boride nanostructures*. Vol. 80. 13 vols. *PHYSICAL REVIEW B*.
- Tayebi, N., and F. Shojaie. 2021. "Detection of Cyanogen Halides by B36 Nanocluster: DFT Study." *Physical Chemistry Research* 9 (1).
- Vessally, E., S. A. Javarsineh, A. Bekhradnia, A. Hosseinian, and S. Ahmadi. 2020. "Computational study of a B36 borophene as an electronic sensor for the anticancer drug Cisplatinium." *Journal of Computational Electronics* 20 (1).
- Wang, L., F. Zhang, and C. Lin. 2014. Edited by 3724. Vol. 8. *ACS Nano* .
- Wang, Z., Lü, T., Wang, H., Feng, Y. P., & Zheng, J. (2017). New crystal structure prediction of fully hydrogenated borophene by first principles calculations. *Scientific Reports*, 7(1). doi:10.1038/s41598-017-00667-x. tarih yok.
- Wang, Z., T. Lü, H. Wang, Y. P. Feng, and J. Zheng. 2017. *New crystal structure prediction of fully hydrogenated borophene by first principles calculations*. Vol. 7. 1 vols. *Scientific Reports*.

- Wang, Z., T. Lü, H. Wang, Y. P. Feng, and J. Zheng. 2017. "New crystal structure prediction of fully hydrogenated borophene by first principles calculations." *Scientific Reports* 7 (1).
- Wang, Z., T. Lü, H. Wang, Y. P. Feng, and J. Zheng. 2017. "New crystal structure prediction of fully hydrogenated borophene by first principles calculations." *Scientific Reports* 7 (1).
- Wang, Z., T. Lü, H. Wang, Y. P. Feng, and J. Zheng. 2019. "Review of borophene and its potential applications." *Frontiers of Physics* 14 (3).
- Wu, R., I. K. Drozdov, S. Eltinge, P. Zahl, I. S. Beigi, I. Božović, and A. Gozar. 2019. "Large-area single-crystal sheets of borophene on Cu(111) surfaces." *Nat Nanotechnol* 14 (1).
- Xiao, C., K. Ma, G. Cai, X. Zhang, and E. Vessally. 2020. "Borophene as an electronic sensor for Metronidazole Drug: A computational study." *Journal of Molecular Graphics and Modelling*, 96.
- Xiao, H., W. Cao, T. Ouyang, S. Guo, C. He, and J. Zhong. 2017. "Lattice thermal conductivity of borophene from First Principle Calculation." *Scientific Reports* 7 (1).
- Xu, L., A. Du, and L. Kou. 2016. *Hydrogenated borophene as a stable twodimensional Dirac material with an ultrahigh Fermi velocity*. Vol. 18. 39 vols. Physical Chemistry Chemical Physics.
- Zhong, Q., L. Kong, J. Gou, W. Li, S. Sheng, S. Yang, P. Cheng, H. Li, K. Wu, and L. Chen. 2017. "Synthesis of borophene nanoribbons on Ag(110) surface." *Phys. Rev. Mater.* 1 (2).
- Zhou, H., Y. Cai, G. Zhang, and Y. Zhang. 2017. "Superior lattice thermal conductance of single-layer borophene." *Npj 2D Materials and Applications* 1 (14).
- URL1. <https://app.biorender.com/biorender/templates/figures/5c8c7ba6d4f2ef3300632941/t-60d4917167f1d600a4493099amino-acid-chart> Copyright 2022 by BioRender



# APPENDIX A

GLY-EDGE-CO

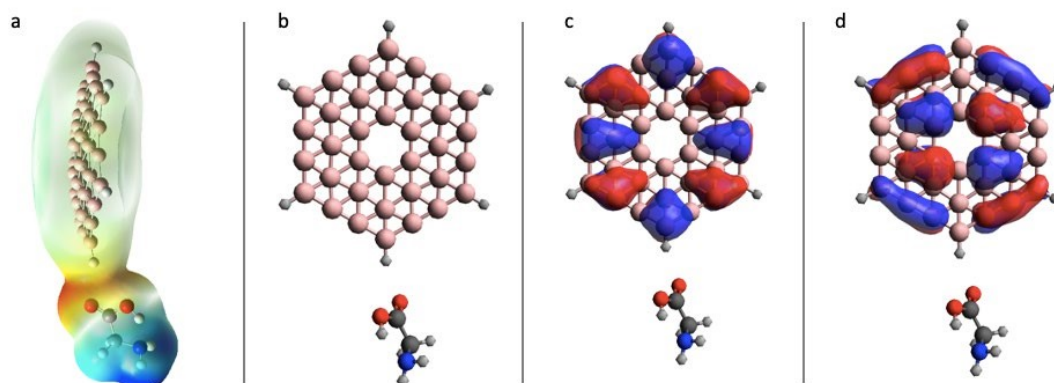


Figure A.1 B<sub>36</sub>H<sub>6</sub> - Glycine - Edge - CO complex's a)EPS surface b)structure c)HOMO d)LUMO

GLY-EDGE-NH<sub>2</sub>

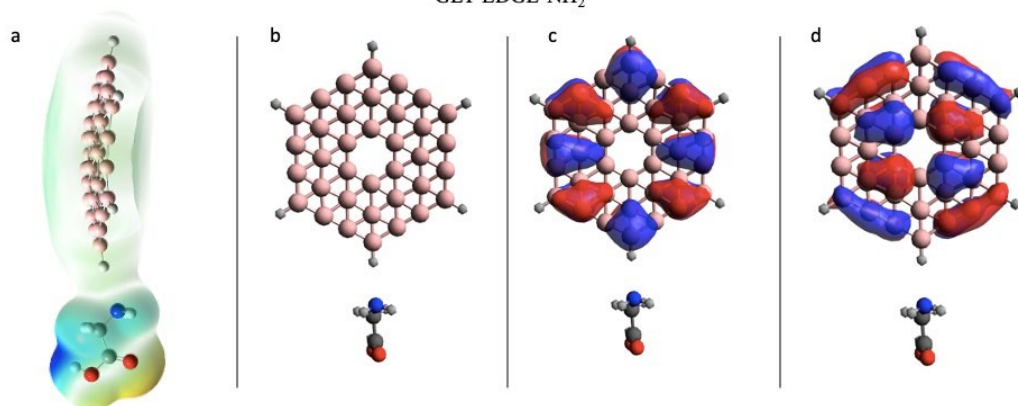


Figure A.2 B<sub>36</sub>H<sub>6</sub> - Glycine - Edge - NH<sub>2</sub> complex's a)EPS surface b)structure c)HOMO d)LUMO

GLY-EDGE-R

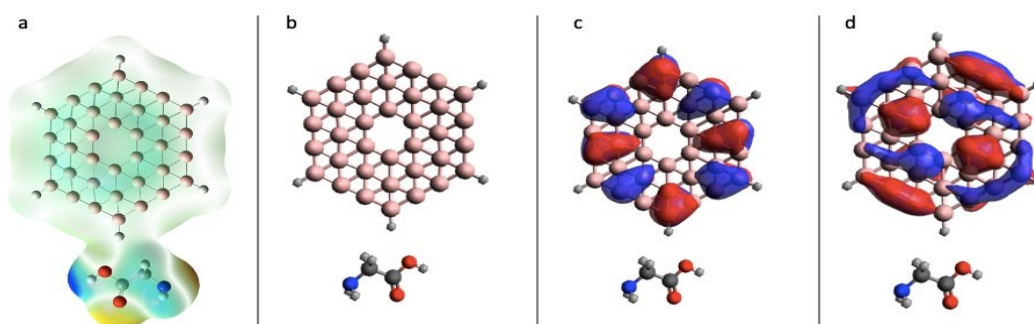


Figure A.3 B<sub>36</sub>H<sub>6</sub> - Glycine - Edge - R complex's a)EPS surface b)structure c)HOMO d)LUMO

GLY-TOP - CO

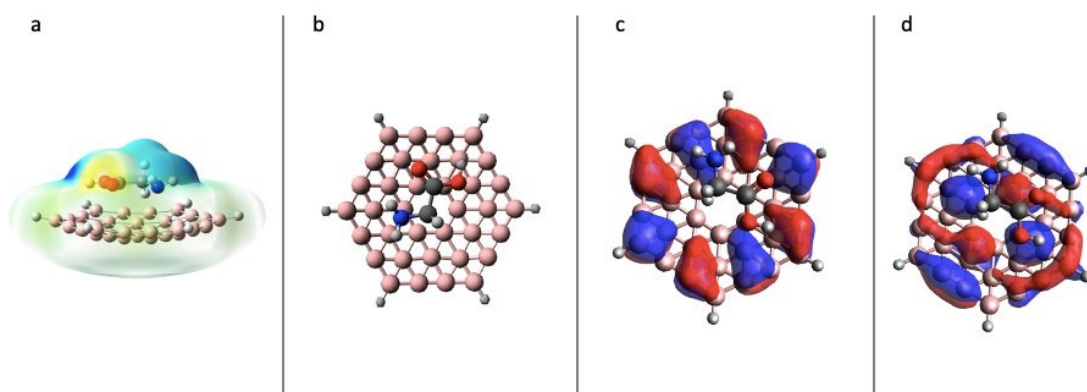


Figure A.4 B<sub>36</sub>H<sub>6</sub> - Glycine - Top - CO complex's a)EPS surface b)structure c)HOMO d)LUMO

GLY-TOP -NH<sub>2</sub>

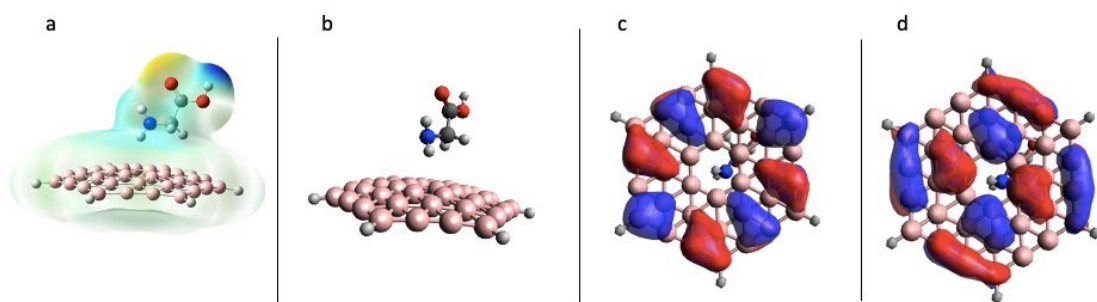


Figure A.5 B<sub>36</sub>H<sub>6</sub> - Glycine - Top - NH<sub>2</sub> complex's a)EPS surface b)structure c)HOMO d)LUMO

GLY-TOP -R

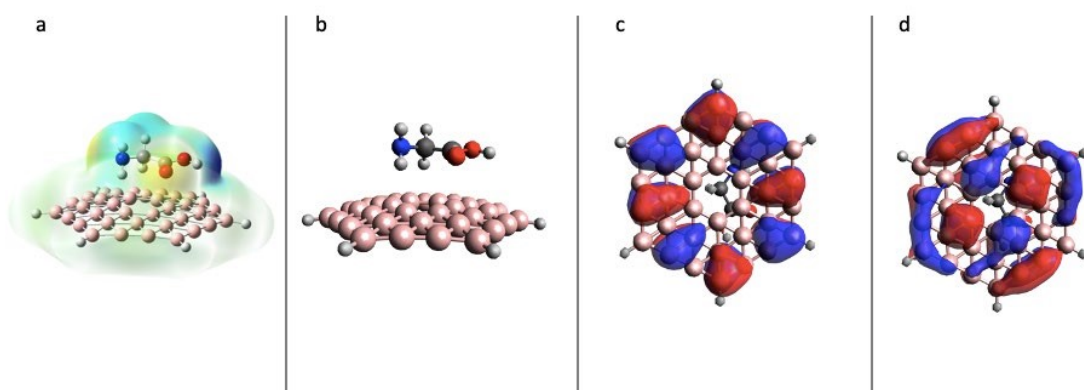


Figure A.6 B<sub>36</sub>H<sub>6</sub> - Glycine - Top - R complex's a)EPS surface b)structure c)HOMO d)LUMO

GLY- BOTTOM - CO

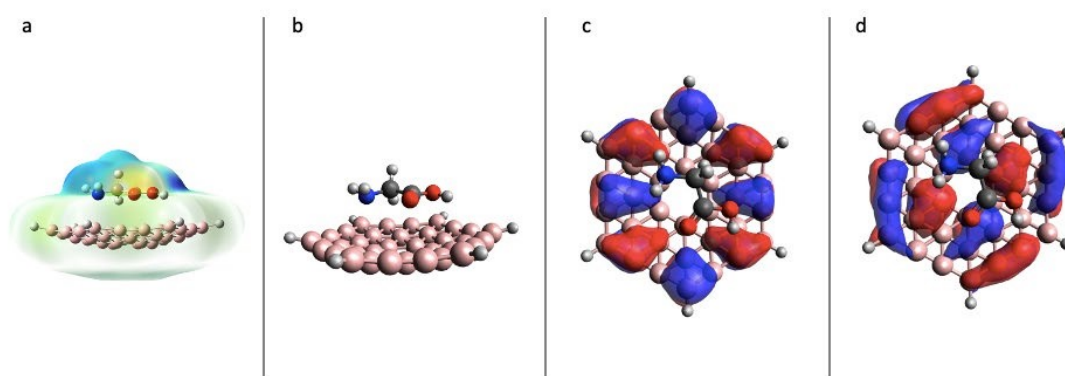


Figure A.7 B<sub>36</sub>H<sub>6</sub> - Glycine - Bottom - CO complex's a)EPS surface b)structure c)HOMO d)LUMO

GLY - BOTTOM - NH2

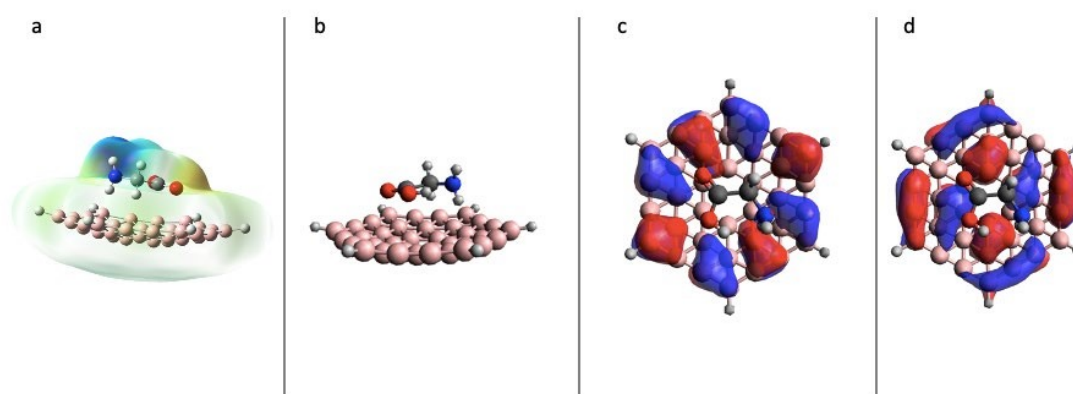


Figure A.8 B<sub>36</sub>H<sub>6</sub> - Glycine - Bottom - NH<sub>2</sub> complex's a)EPS surface b)structure c)HOMO d)LUMO

GLY - BOTTOM - R

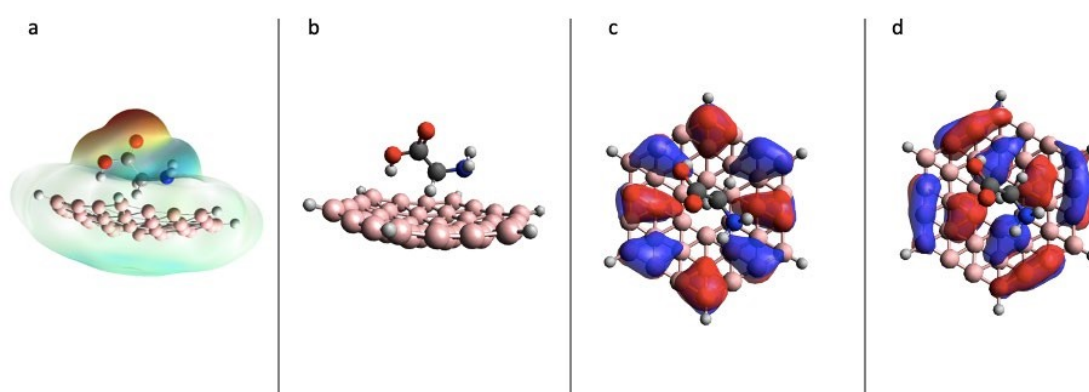


Figure A.9 B<sub>36</sub>H<sub>6</sub> - Glycine - Bottom - R complex's a)EPS surface b)structure c)HOMO d)LUMO

TYR-EDGE-CO

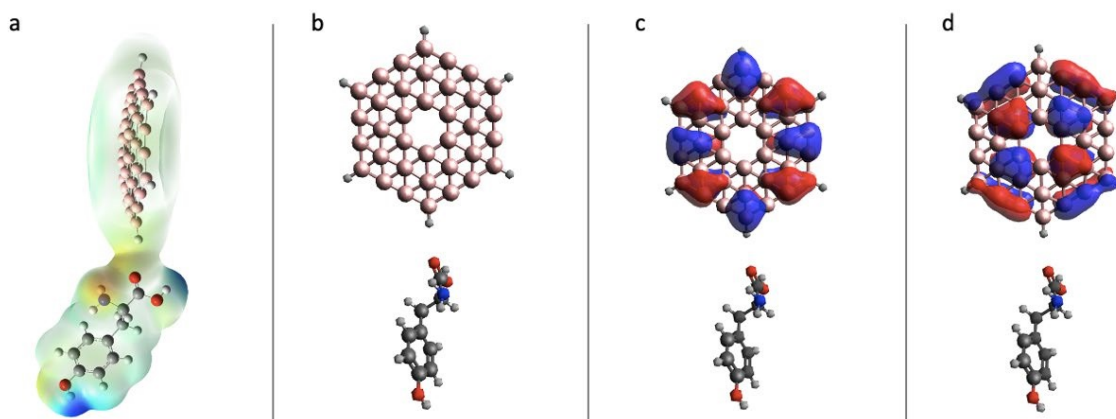


Figure A.10 B<sub>36</sub>H<sub>6</sub> - Tyrosine - Edge - CO complex's a)EPS surface b)structure c)HOMO d)LUMO

TYR-EDGE-NH<sub>2</sub>

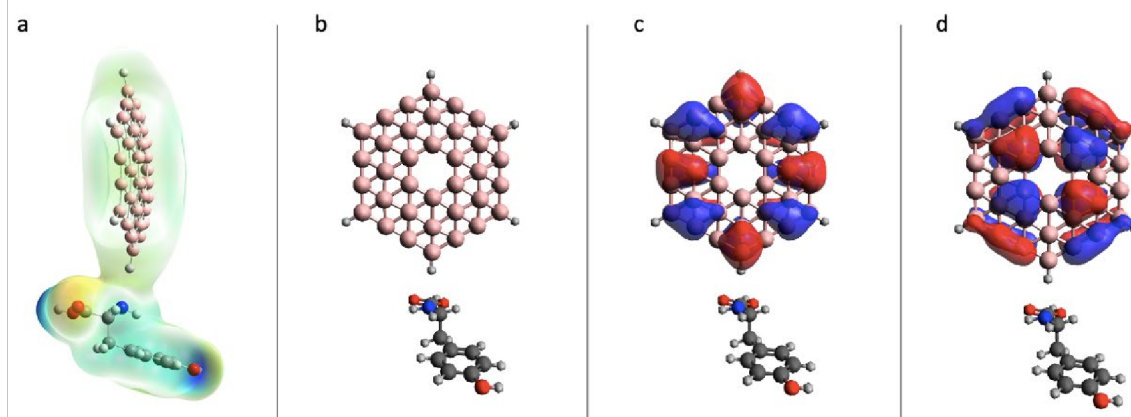


Figure A.11 B<sub>36</sub>H<sub>6</sub> - Tyrosine - Edge - NH<sub>2</sub> complex's a)EPS surface b)structure c)HOMO d)LUMO

TYR-EDGE-R

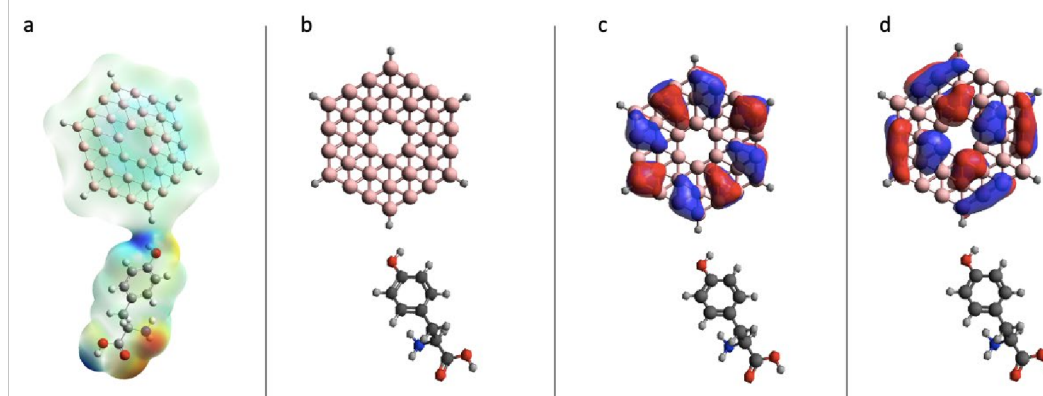


Figure A.12 B<sub>36</sub>H<sub>6</sub> - Tyrosine - Edge - R complex's a)EPS surface b)structure c)HOMO d)LUMO

TYR-TOP-CO

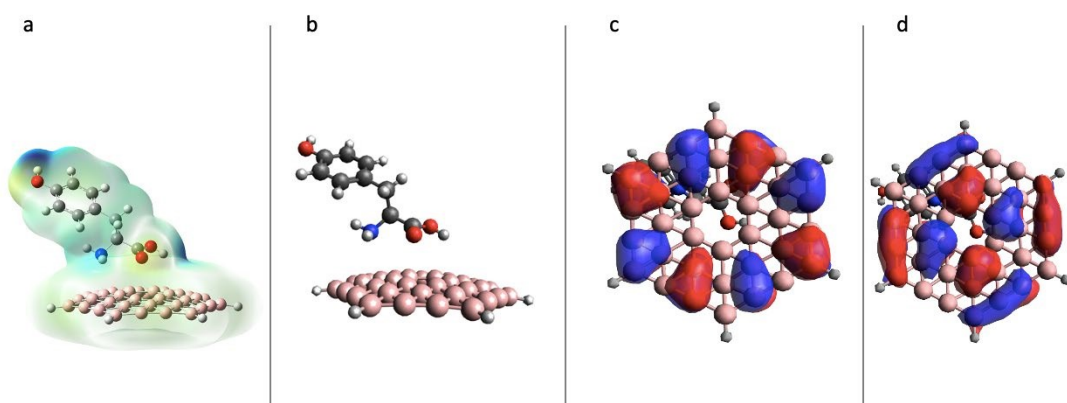


Figure A.13 B<sub>36</sub>H<sub>6</sub> - Tyrosine - Top - CO complex's a)EPS surface b)structure c)HOMO d)LUMO

TYR-TOP-NH2

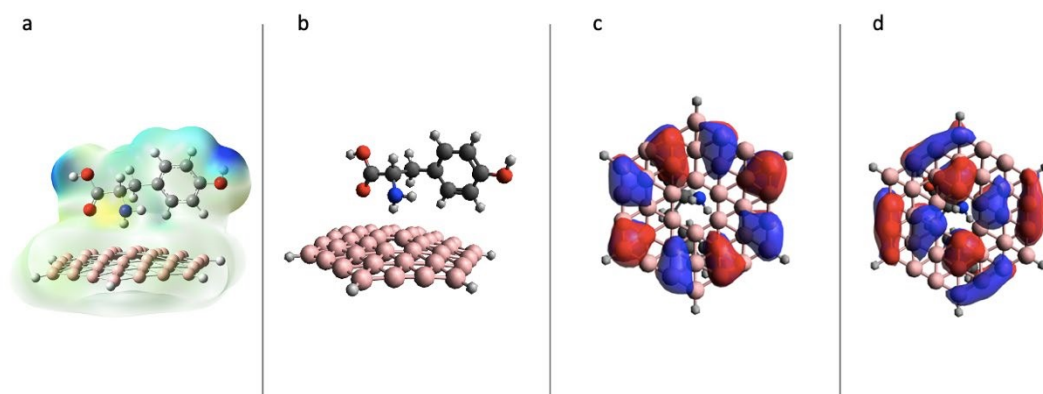


Figure A.14 B<sub>36</sub>H<sub>6</sub> - Tyrosine - Top - NH<sub>2</sub> complex's a)EPS surface b)structure c)HOMO d)LUMO

TYR-TOP-R

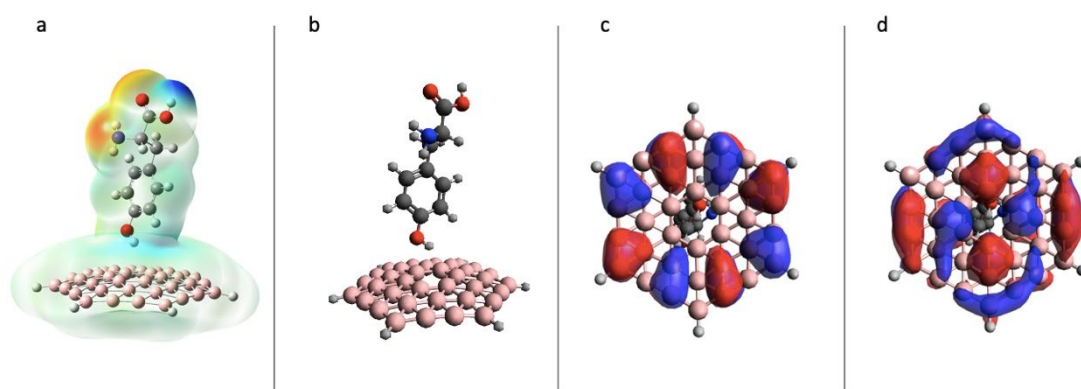


Figure A.15 B<sub>36</sub>H<sub>6</sub> - Tyrosine - Top - R complex's a)EPS surface b)structure c)HOMO d)LUMO

TYR-BOTTOM -CO

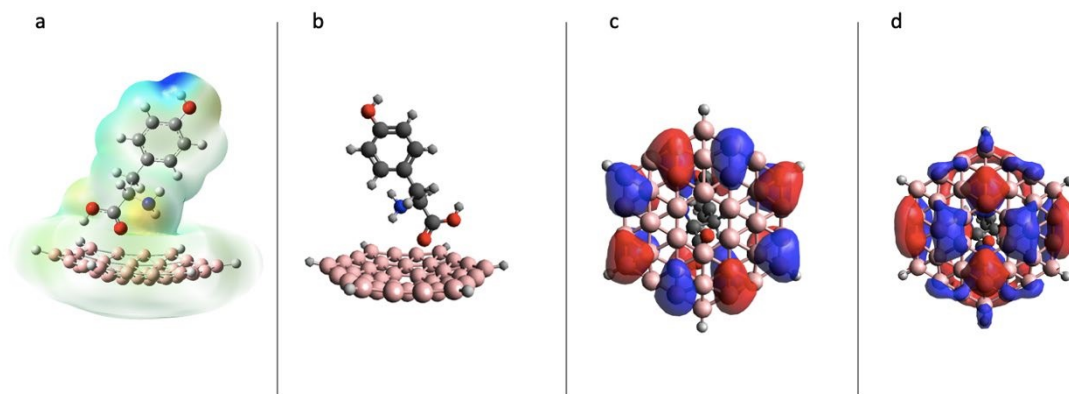


Figure A.16  $B_{36}H_6$  - Tyrosine - Bottom - CO complex's a)EPS surface b)structure c)HOMO d)LUMO

TYR-BOTTOM -NH2

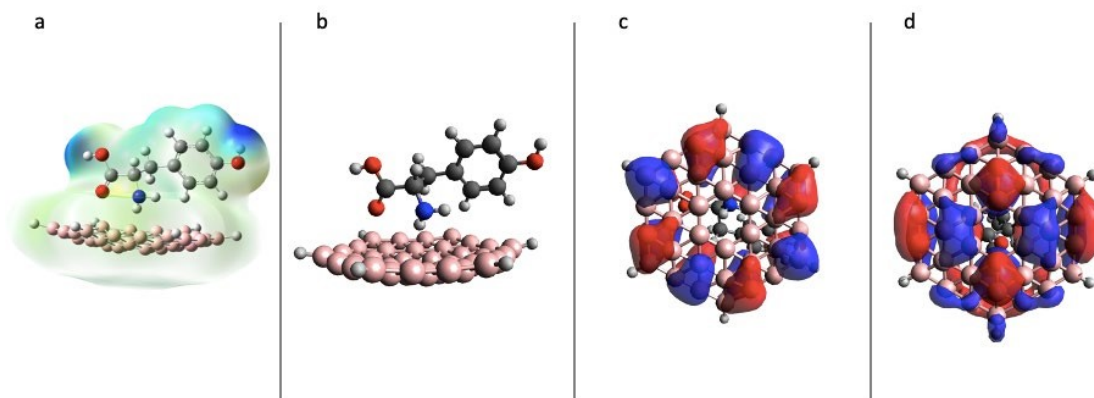


Figure A.17  $B_{36}H_6$  - Tyrosine - Bottom - NH2 complex's a)EPS surface b)structure c)HOMO d)LUMO

TYR-BOTTOM - R

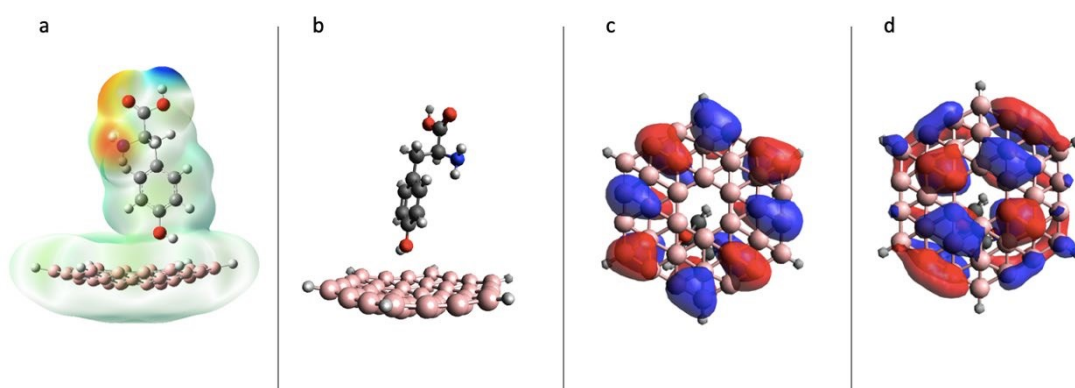


Figure A.18  $B_{36}H_6$  - Tyrosine - Bottom - R complex's a)EPS surface b)structure c)HOMO d)LUMO

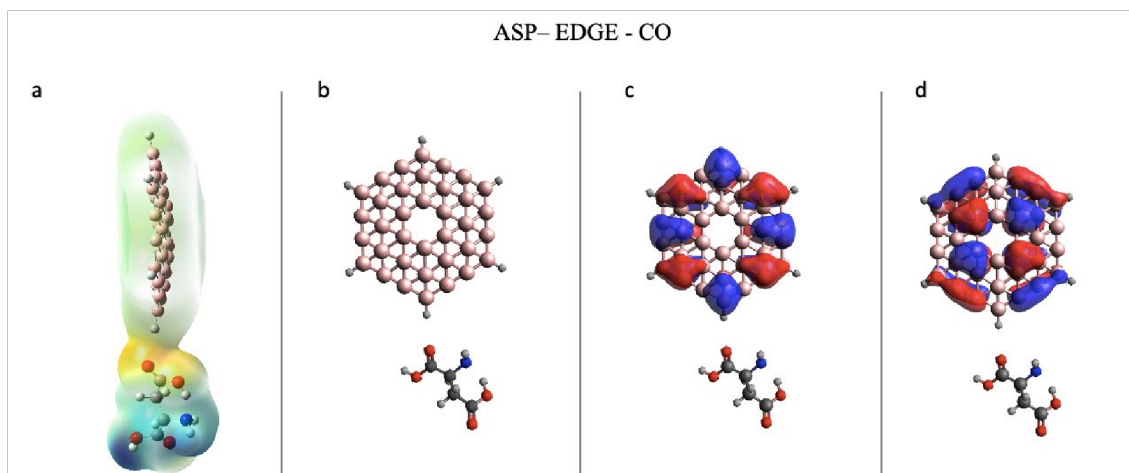


Figure A.19  $B_{36}H_6$  - Aspartic Acid - Edge-CO complex's a)EPS surface b)structure c)HOMO  
d)LUMO

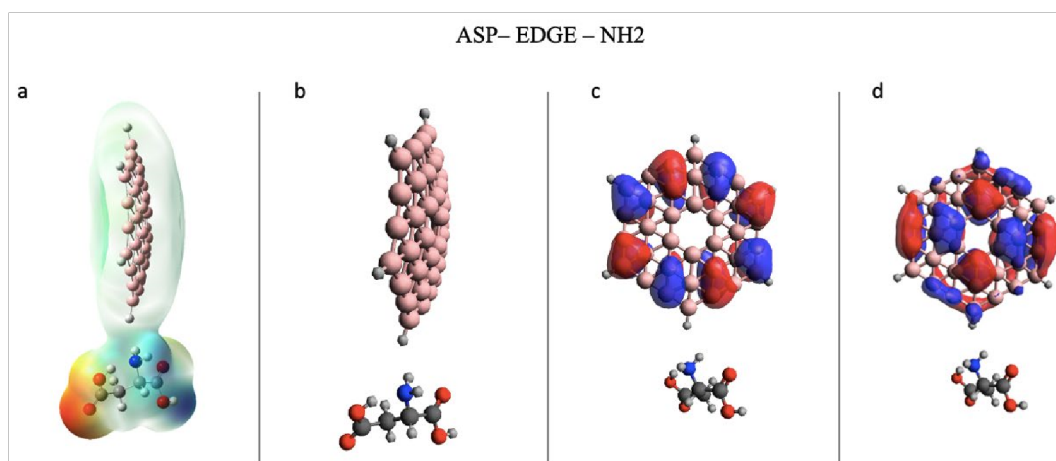


Figure A.20  $B_{36}H_6$  - Aspartic Acid - Edge-NH2 complex's a)EPS surface b)structure c)HOMO  
d)LUMO

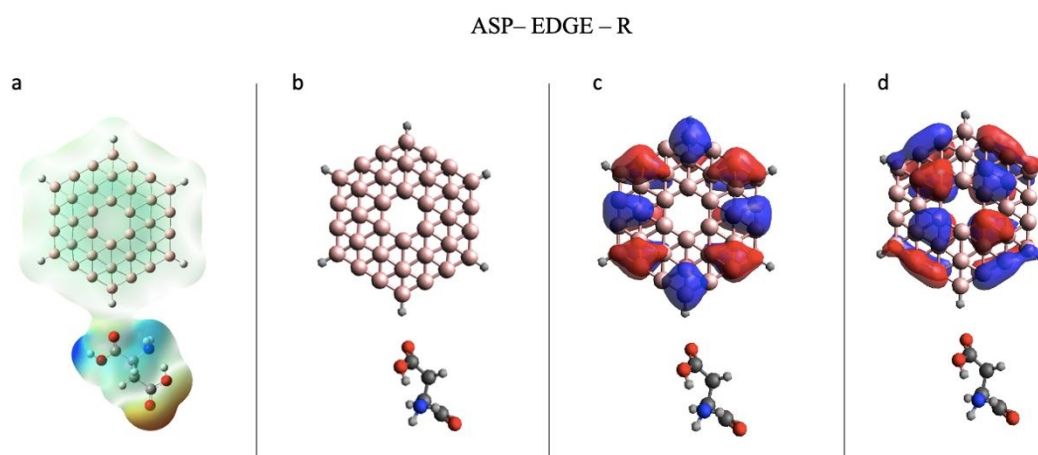


Figure A.21  $B_{36}H_6$  - Aspartic Acid - Edge - R complex's a)EPS surface b)structure c)HOMO  
d)LUMO

ASP-TOP-CO

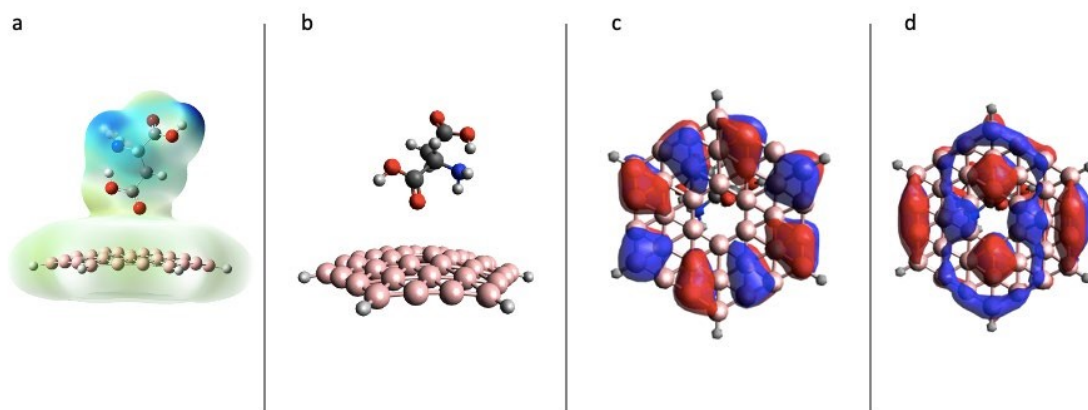


Figure A.22 B<sub>36</sub>H<sub>6</sub> - Aspartic Acid - Top - CO complex's a)EPS surface b)structure c)HOMO d)LUMO

ASP-TOP-NH2

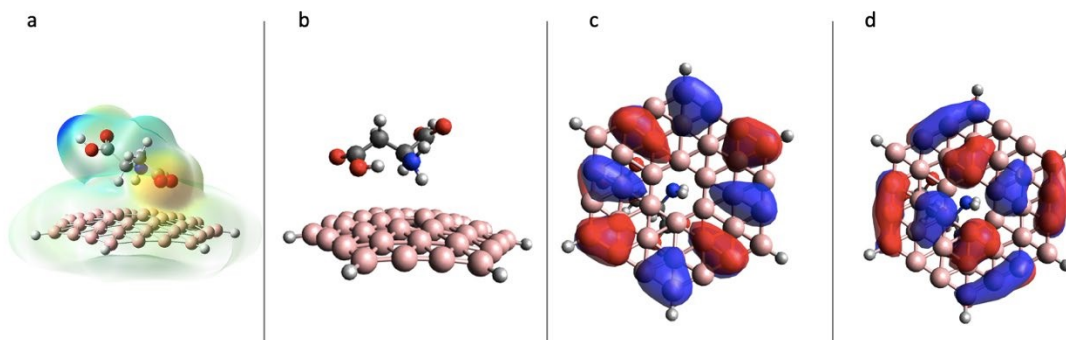


Figure A.23 B<sub>36</sub>H<sub>6</sub> - Aspartic Acid - Top - NH<sub>2</sub> complex's a)EPS surface b)structure c)HOMO d)LUMO

ASP-TOP-R

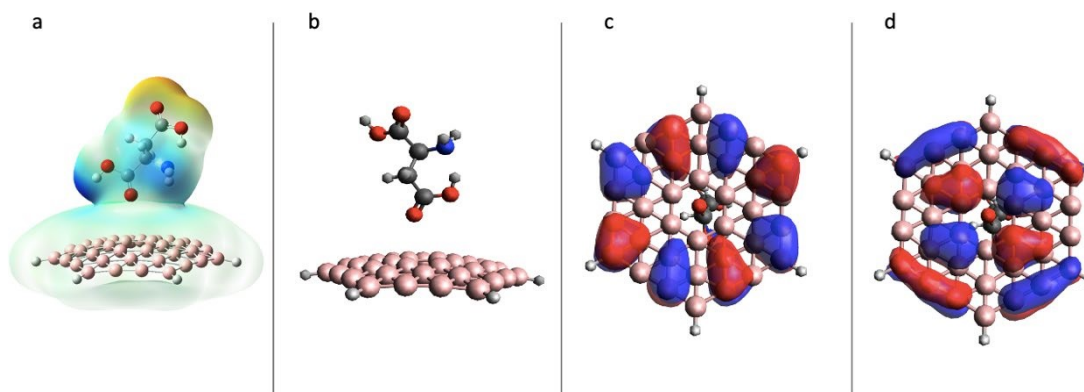


Figure A.24 B<sub>36</sub>H<sub>6</sub> - Aspartic Acid - Top - R complex's a)EPS surface b)structure c)HOMO d)LUMO



ASP- BOTTOM - CO

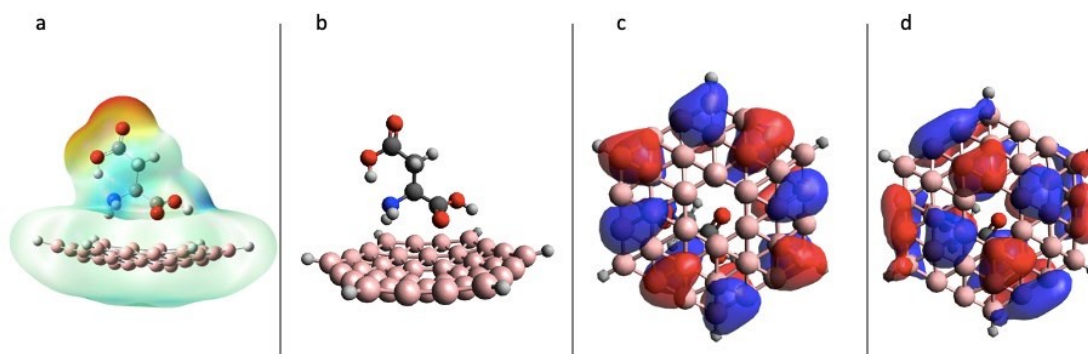


Figure A.25 B<sub>36</sub>H<sub>6</sub> - Aspartic Acid - Bottom-CO complex's a)EPS surface b)structure c)HOMO  
d)LUMO

ASP- BOTTOM - NH2

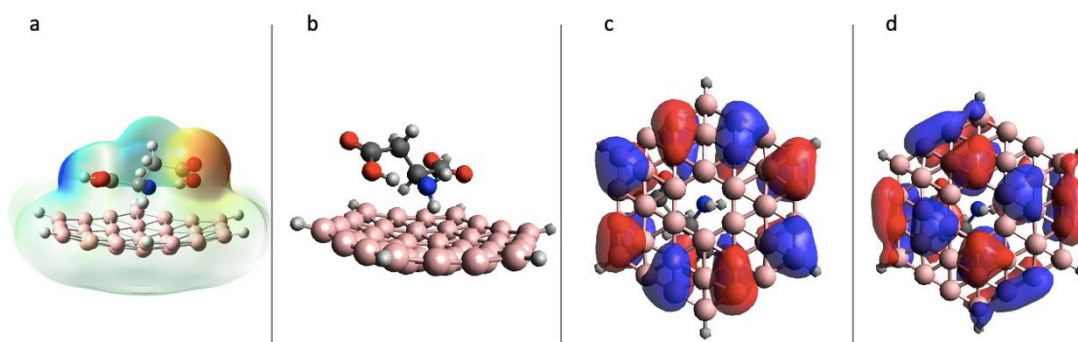


Figure A.26 B<sub>36</sub>H<sub>6</sub> - Aspartic Acid-Bottom-NH<sub>2</sub> complex's a)EPS surface b)structure c)HOMO  
d)LUMO

ASP- BOTTOM - R

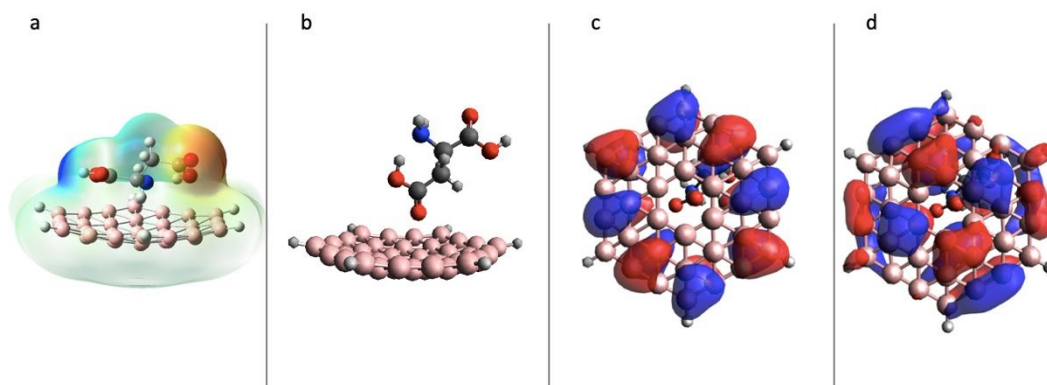


Figure A.27 B<sub>36</sub>H<sub>6</sub> - Aspartic Acid - Bottom - R complex's a)EPS surface b)structure c)HOMO  
d)LUMO

HIS-EDGE-CO

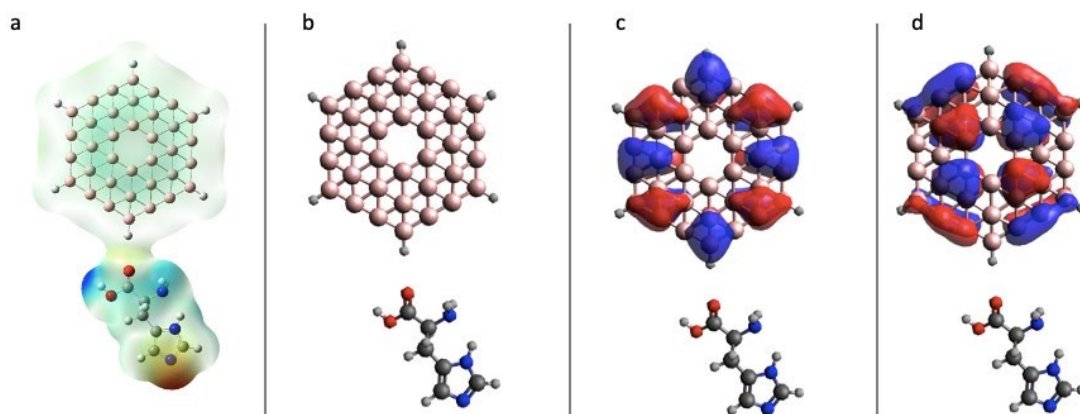


Figure A.28  $B_{36}H_6$  - Histidine - Edge - CO complex's a)EPS surface b)structure c)HOMO d)LUMO

HIS-EDGE-NH2

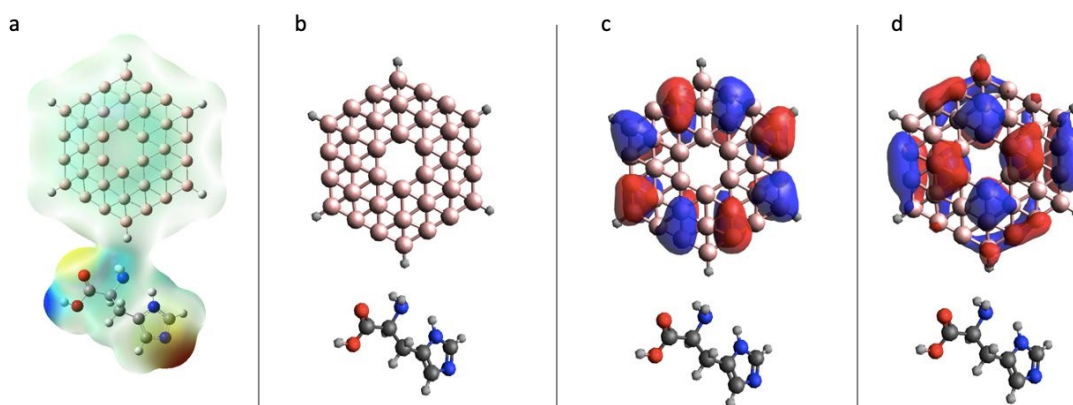


Figure A.29  $B_{36}H_6$  - Histidine - Edge - NH2 complex's a)EPS surface b)structure c)HOMO d)LUMO

HIS-EDGE-R

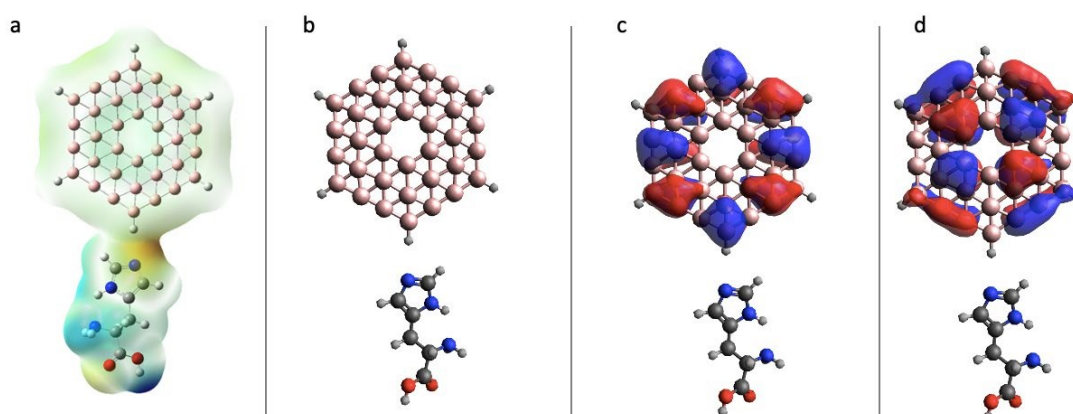


Figure A.30  $B_{36}H_6$  - Histidine - Edge - R complex's a)EPS surface b)structure c)HOMO d)LUMO

HIS - TOP - CO

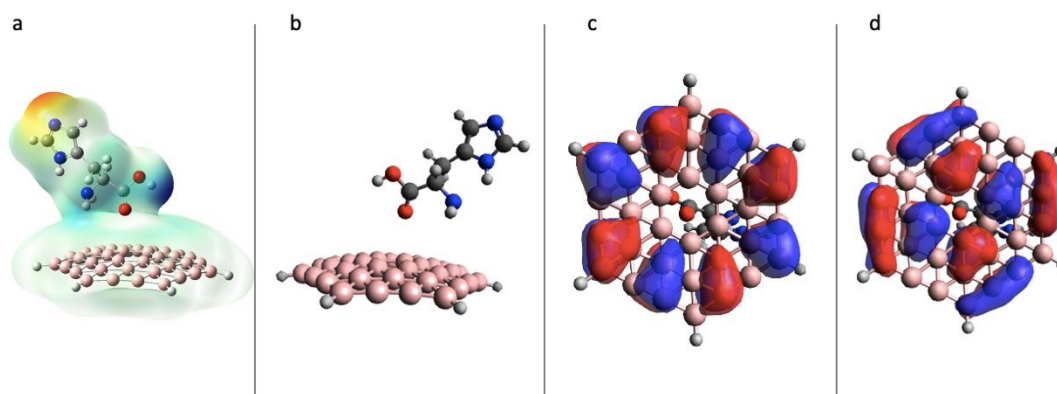


Figure A.31 B<sub>36</sub>H<sub>6</sub> - Histidine - Top - CO complex's a)EPS surface b)structure c)HOMO d)LUMO

HIS - TOP - NH2

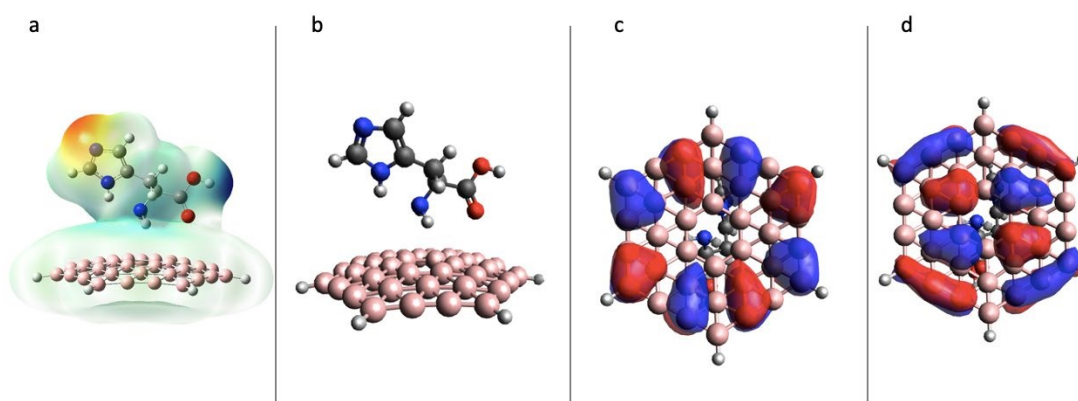


Figure A.32 B<sub>36</sub>H<sub>6</sub> - Histidine - Top - NH<sub>2</sub> complex's a)EPS surface b)structure c)HOMO d)LUMO

HIS - TOP - R

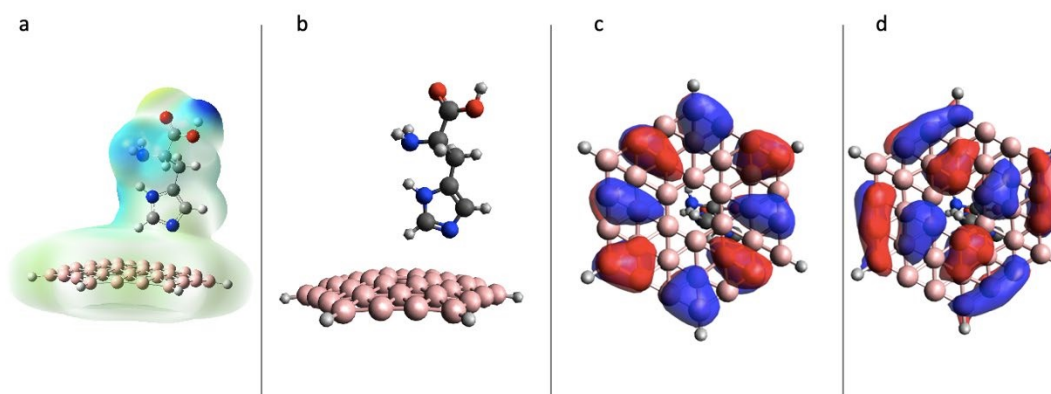


Figure A.33 B<sub>36</sub>H<sub>6</sub> - Histidine - Top - R complex's a)EPS surface b)structure c)HOMO d)LUMO

HIS – BOTTOM - CO

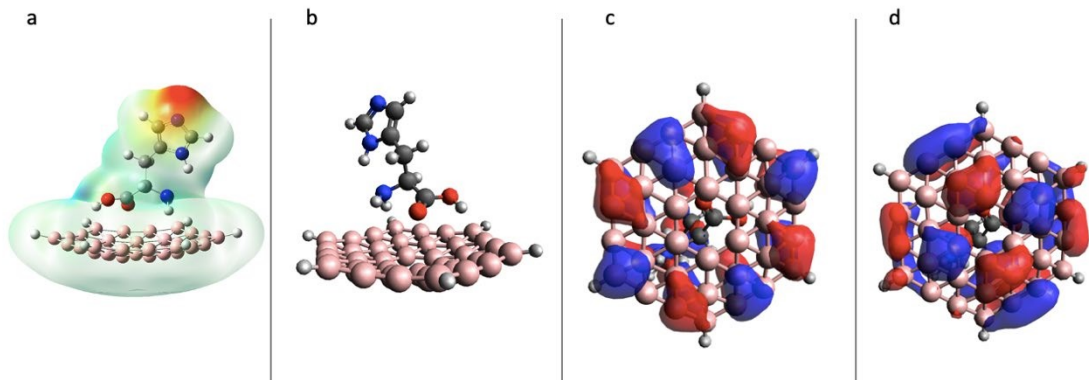


Figure A.34  $B_3H_6$  - Histidine - Bottom - CO complex's a)EPS surface b)structure c)HOMO  
d)LUMO

HIS – BOTTOM – NH2

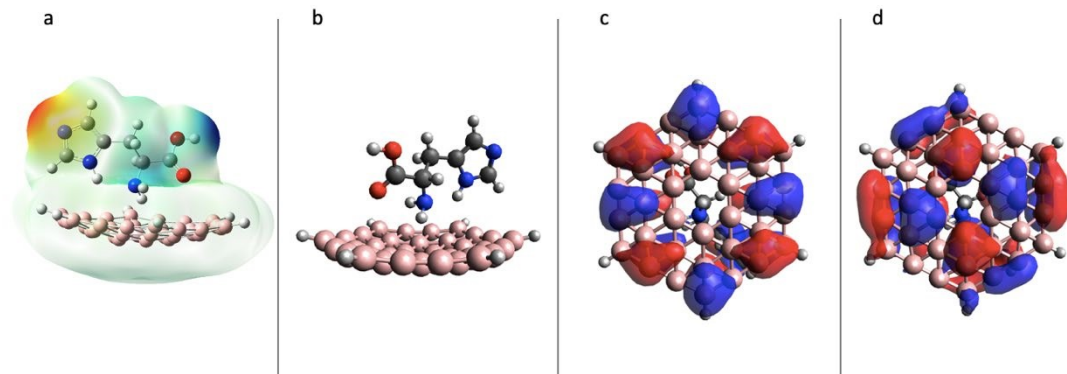


Figure A.35  $B_3H_6$  - Histidine - Bottom - NH2 complex's a)EPS surface b)structure c)HOMO  
d)LUMO

HIS – BOTTOM - R

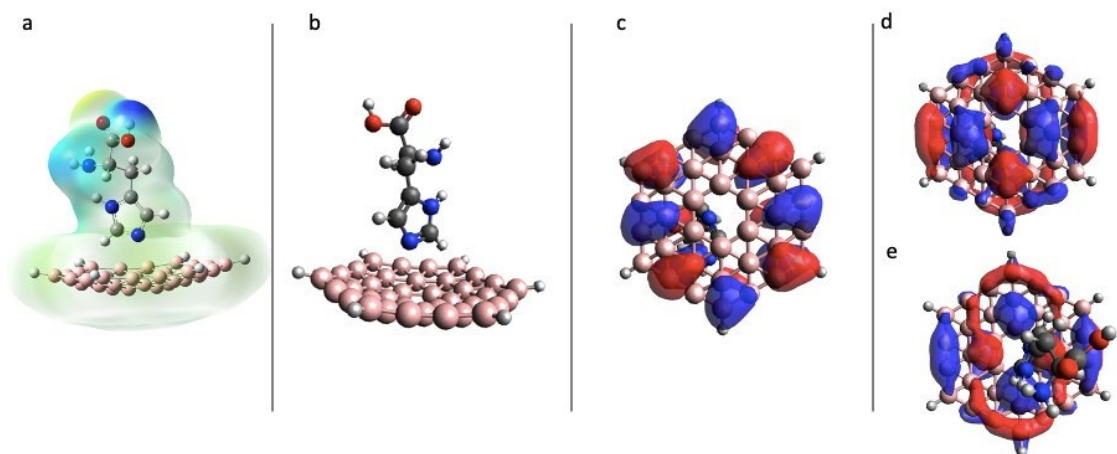


Figure A.36  $B_3H_6$  - Histidine - Bottom - R complex's a)EPS surface b)structure c)HOMO d)LUMO  
and  
e) LUMO from different angles

## APPENDIX B Calculation result tables (excluded versions)

### 1. B<sub>36</sub>H<sub>6</sub> - GLYCINE COMPLEXES

	Position	Orientation	Zero-point correction (kJ/mol)	Zero-point Corrected Energies (kJ/mol)	Relative Energies (kJ/mol)
<b>G l y c i n e</b>	<b>Edge</b>	-Co	742,74375	-3104244,864	67,486125
		-NH2	740,8275	-3104225,946	86,4045
		-R	741,040125	-3104245,371	66,9795
	<b>Top</b>	-Co	743,3055	-3104310,744	1,6065
		-NH2	744,6495	-3104262,664	49,686
		-R	744,69675	-3104290,851	21,49875
	<b>Bottom</b>	-Co	743,817375	-3104312,35	0
		-NH2	741,785625	-3104289,329	23,02125
		-R	743,484	-3104275,511	36,83925

Table B.1 Energy values for complexes of Glycine

	Position	Orientation	E homo (eV)	E lumo (eV)	Complex Band Gap (eV)	ΔBG (eV)	%ΔBG (eV)
<b>G l y c i n e</b>	<b>Edge</b>	-Co	-5,585	-3,373	2,212	-0,106	-4,574
		-NH2	-5,755	-3,541	2,214	-0,104	-4,484
		-R	-5,814	-3,589	2,226	-0,155	-6,669
	<b>Top</b>	-Co	-5,712	-3,541	2,171	-0,147	-6,360
		-NH2	-5,847	-3,616	2,231	-0,087	-3,769
		-R	-5,802	-3,567	2,235	-0,083	-3,576
	<b>Bottom</b>	-Co	-5,698	-3,511	2,187	-0,131	-5,660
		-NH2	-5,757	-3,578	2,180	-0,139	-5,978
		-R	-5,914	-3,775	2,140	-0,179	-7,703

Table B.2 Homo – Lumo Energy values for complexes of Glycine

## 2. B<sub>36</sub>H<sub>6</sub> - TYROSINE COMPLEXES

	Position	Orientation	Zero-point correction (kJ/mol)	Zero-point Corrected Energies (kJ/mol)	Relative Energies (kJ/mol)
T y r o s i n e	Edge	-Co	1039,2165	-4011393,577	73,192875
		-NH2	1040,529	-4011398,228	68,541375
		-R	1039,71525	-4011394,152	72,618
	Top	-Co	1041,996375	-4011443,166	23,604
		-NH2	1042,762875	-4011450,521	16,24875
		-R	1041,450375	-4011418,706	48,06375
	Bottom	-Co	1039,450125	-4011438,824	27,94575
		-NH2	1042,92825	-4011466,77	0
		-R	1039,878	-4011421,701	45,068625

Table B.3 Energy values for complexes of Tyrosine.

	Position	Orientation	E homo (eV)	E lumo (eV)	Complex Band Gap (eV)	ΔBG (eV)	%ΔBG (eV)
T y r o s i n e	Edge	-Co	-5,701	-3,479	2,222	-0,096	-4,153
		-NH2	-5,652	-3,442	2,210	-0,108	-4,662
		-R	-5,889	-3,662	2,226	-0,092	-3,966
	Top	-Co	-5,651	-3,414	2,237	-0,081	-3,502
		-NH2	-5,672	-3,427	2,245	-0,074	-3,178
		-R	-5,897	-3,681	2,216	-0,102	-4,396
	Bottom	-Co	-5,711	-3,555	2,155	-0,163	-7,029
		-NH2	-5,617	-3,436	2,182	-0,137	-5,905
		-R	-5,854	-3,663	2,191	-0,127	-5,482

Table B.4 Homo – Lumo Energy values for complexes of Tyrosine.

### 3. B<sub>36</sub>H<sub>6</sub> - ASPARTIC ACID COMPLEXES

	Position	Orientation	Zero-point correction (kJ/mol)	Zero-point Corrected Energies (kJ/mol)	Relative Energies (kJ/mol)
A s p a r t i c A c i d	Edge	-Co	858,640125	-3702534,056	71,486625
		-NH2	858,624375	-3702533,363	72,179625
		-R	858,766125	-3702537,253	68,289375
	Top	-Co	856,7265	-3702545,427	60,115125
		-NH2	860,66925	-3702588,183	17,359125
		-R	857,611125	-3702556,778	48,764625
Bottom	-Co	859,20975	-3702587,844	17,69775	
	-NH2	861,627375	-3702605,542	0	
	-R	857,794875	-3702572,047	33,495	

Table B.5 Energy values for complexes of Aspartic Acid.

	Position	Orientation	E homo (eV)	E lumo (eV)	Complex Band Gap (eV)	ΔBG (eV)	%ΔBG (eV)
A s p a r t i c A c i d	Edge	-Co	-5,595	-3,381	2,214	-0,104	-4,500
		-NH2	-5,902	-3,676	2,225	-0,093	-4,025
		-R	-5,852	-3,630	2,222	-0,096	-4,160
	Top	-Co	-5,515	-3,252	2,263	-0,055	-2,373
		-NH2	-5,820	-3,632	2,187	-0,131	-5,648
		-R	-5,907	-3,667	2,239	-0,079	-3,420
Bottom	-Co	-6,064	-3,880	2,184	-0,134	-5,799	
	-NH2	-5,872	-3,710	2,162	-0,157	-6,766	
	-R	-5,529	-3,335	2,194	-0,124	-5,365	

Table B.6 Homo – Lumo Energy values for complexes of Aspartic Acid

#### 4. B<sub>36</sub>H<sub>6</sub> - HISTIDINE COMPLEXES

	Position	Orientation	Zero-point correction (kJ/mol)	Zero-point Corrected Energies (kJ/mol)	Relative Energies (kJ/mol)
H i s t i d i n e	Edge	-Co	954,156	-3798142,218	56,849625
		-NH <sub>2</sub>	953,596875	-3798141,635	57,432375
		-R	954,62325	-3798146,494	52,5735
	Top	-Co	951,888	-3798160,404	38,663625
		-NH <sub>2</sub>	955,523625	-3798179,243	19,824
		-R	956,914875	-3798180,797	18,27
	Bottom	-Co	954,61275	-3798199,067	0
		-NH <sub>2</sub>	956,15625	-3798199,065	0,002625001
		-R	954,303	-3798189,032	10,03275

Table B.7 Energy values for complexes of Histidine.

	Position	Orientation	E homo (eV)	E luno (eV)	Complex Band Gap (eV)	ΔBG (eV)	%ΔBG (eV)
H i s t i d i n e	Edge	-Co	-5,818	-3,597	2,220	-0,098	-4,230
		-NH <sub>2</sub>	-5,888	-3,666	2,222	-0,097	-4,175
		-R	-5,621	-3,407	2,214	-0,105	-4,525
	Top	-Co	-5,872	-3,632	2,240	-0,078	-3,372
		-NH <sub>2</sub>	-5,876	-3,663	2,214	-0,105	-4,515
		-R	-5,568	-3,342	2,225	-0,093	-4,012
	Bottom	-Co	-5,980	-3,805	2,175	-0,143	-6,187
		-NH <sub>2</sub>	-5,871	-3,707	2,164	-0,155	-6,669
		-R	-5,583	-3,404	2,179	-0,139	-6,002

Table B.8 Homo – Lumo Energy values for complexes of Histidine.



## 5. B<sub>36</sub>H<sub>6</sub> - Amino Acid Distances

	Amino Acids				
	Distance between atoms	GLY	TYR	ASP	HIS
E D G E	B --- Oc (Å)	3,535	3,775	3,691	3,687
	B --- N (Å)	3,707	3,683	3,901	3,847
	B --- R (Å)	3,642	3,834	3,591	3,616
T O P	COA --- Oc (Å)	3,635	3,907	3,633	3,611
	COA --- N (Å)	3,545	3,471	3,64	3,591
	COA --- R (Å)	2,713	3,414	3,371	4,074
B O T T O M	COA --- Oc (Å)	2,93	2,449	2,476	2,397
	COA --- N (Å)	3,445	2,58	2,527	2,424
	COA --- R (Å)	1,465	3,145	2,276	2,522

Table B.9 Distance between B<sub>36</sub>H<sub>6</sub> and amino acids for each complex.